PROTEINS
STRUCTURE ■ FUNCTION ■ BIOINFORMATICS

Molecular determinants of the pK_a values of Asp and Glu residues in staphylococcal nuclease

Carlos A. Castañeda,[1] Carolyn A. Fitch,[1] Ananya Majumdar,[2] Victor Khangulov,[1] Jamie L. Schlessman,[3] and Bertrand E. García-Moreno[1]*

[1] Department of Biophysics, The Johns Hopkins University, Baltimore, Maryland 21218
[2] Biomolecular NMR Facility, The Johns Hopkins University, Baltimore, Maryland 21218
[3] Department of Chemistry, United States Naval Academy, Annapolis, Maryland 21402

ABSTRACT

Prior computational studies of the acid-unfolding behavior of staphylococcal nuclease (SNase) suggest that the pK_a values of its carboxylic groups are difficult to reproduce with electrostatics calculations with continuum methods. To examine the molecular determinants of the pK_a values of carboxylic groups in SNase, the pK_a values of all 20 Asp and Glu residues were measured with multidimensional and multinuclear NMR spectroscopy in an acid insensitive variant of SNase. The crystal structure of the protein was obtained to describe the microenvironments of the carboxylic groups. Fourteen Asp and Glu residues titrate with relatively normal pK_a values that are depressed by less than 1.1 units relative to the normal pK_a of Asp and Glu in water. Only six residues have pK_a values shifted by more than 1.5 units. Asp-21 has an unusually high pK_a of 6.5, which is probably the result of interactions with other carboxylic groups at the active site. The most perturbed pK_a values appear to be governed by hydrogen bonding and not by Coulomb interactions. The pK_a values calculated with standard continuum electrostatics methods applied to static structures are more depressed than the measured values because Coulomb effects are exaggerated in the calculations. The problems persist even when the protein is treated with the dielectric constant of water. This can be interpreted to imply that structural relaxation is an important determinant of the pK_a values; however, no major pH-sensitive conformational reorganization of the backbone was detected using NMR spectroscopy.

Proteins 2009; 77:570–588.

Key words: staphylococcal nuclease; NMR; dynamics; pK_a values; electrostatics.

INTRODUCTION

Surface ionizable groups in proteins play essential roles in many biological processes.[1–4] To understand how ionizable groups contribute to function, it is necessary to know their pK_a values and to understand their molecular determinants. Toward this end, the pK_a values of many ionizable groups have been measured with NMR spectroscopy,[5,6] and computational methods for structure-based calculation of pK_a values have been developed to examine their molecular determinants.[7–16] In general, the pK_a values measured with NMR spectroscopy are quite similar to the normal pK_a values of model compounds in water. The reasons that the pK_a values of surface residues are so normal are not well understood; this is not easy to reproduce with structure-based calculations.[17] To examine this problem in detail, the molecular determinants of the pK_a values of Asp and Glu residues in staphylococcal nuclease (SNase) were studied with NMR spectroscopy.

SNase is ideally suited to study the determinants of electrostatic effects in proteins because it is a highly charged protein in which the problems inherent to methods for structure-based pK_a calculations are amplified. Previous attempts to reproduce the acid-unfolding behavior of SNase with standard continuum electrostatics calculations failed.[17] The problem is that overall, the calculated pK_a values are too depressed because Coulomb effects are exaggerated in the calculations with static structures, even when the protein is treated artificially with high dielectric constants. The failure is not subtle: direct potentiometric experiments show that 6.7 H^+ are bound preferentially by the unfolded state during the acid-unfolding

Additional Supporting Information may be found in the online version of this article.
Abbreviations: NMR, nuclear magnetic resonance; SNase, staphylococcal nuclease; δ, chemical shift; Δ+PHS, hyperstable variant of SNase.

Grant sponsors: NSF, Grant number MCB-0743422 (BGME); The Burroughs-Wellcome Fund (CAC); The US Naval Academy John F. Crowley Fellowship (CAC); and DOE Institute of Multi-scale Modeling of Biological Interactions (VK).
*Correspondence to: Bertrand E. García-Moreno, Department of Biophysics, The Johns Hopkins University, 3400 N. Charles St., Baltimore, MD 21218. E-mail: bertrand@jhu.edu
Received 3 December 2008; Revised 18 March 2009; Accepted 20 April 2009
Published online 4 May 2009 in Wiley InterScience (www.interscience.wiley.com).
DOI: 10.1002/prot.22470

transition, whereas according to the calculations, more than 10 H^+ are bound.[17,18]

Several computational methods have been developed previously to improve the agreement between calculated and measured pK_a values.[12–14,17,19] Two of these methods (use of MD simulations to relax the structure and use of arbitrarily high protein dielectric constants) were used to analyze the acid unfolding of SNase, but the improvement between measured and calculated properties was only marginal.[17] The disagreement between measured and calculated pK_a values in other proteins has been interpreted as evidence that the inherent flexibility and conformational relaxation coupled to the ionization of these groups are important determinants of their pK_a values.[12,13,20–22] To examine this possibility in detail, it was necessary to first measure the pK_a values of Asp and Glu residues experimentally.

In this study, the pK_a values of Asp and Glu residues in SNase were measured with multidimensional and multinuclear NMR spectroscopy by monitoring the pH dependence of Cγ (Asp) and Cδ (Glu) resonances.[5] All measurements were performed with a hyperstable variant of SNase known as Δ+PHS, which is stable under acidic conditions.[23] To describe the microenvironments of the acidic groups, the crystal structure of the Δ+PHS nuclease was determined. The salt dependence of pK_a values was measured to examine the magnitude of Coulomb interactions. Contributions from hydrogen bonds were examined by monitoring the pH dependence of H^N chemical shifts of groups near carboxylic groups. The structural consequences of changes in pH on the overall secondary and tertiary structure of the protein were monitored by the H^N, Cα, and Cβ resonances. Structure-based calculations with standard continuum electrostatic methods based on the finite difference solution of the linearized Poisson–Boltzmann (FDPB) equation were used to demonstrate that calculations with a static structure predict pK_a values that are more depressed than the measured values, even when the protein is treated with the dielectric constant of water.

MATERIALS AND METHODS

Protein and peptides

A hyperstable, acid-resistant form of SNase known as Δ+PHS was expressed in *E. coli* BL21/DE3 cells (Invitrogen) transformed with the plasmid Pet24a+. Δ+PHS has five substitutions (G50F, V51N, P117G, H124L, and S128A) and a truncation (residues 44–49). Uniformly $^{13}C/^{15}N$ labeled protein was made by growing *E. coli* in minimal media with $^{15}NH_4Cl$ (1 g/L) and $^{13}C_6$-D-glucose (4 g/L) (Isotec). Δ+PHS was purified following the procedure described previously by Shortle and Meeker.[24] Yields of purified protein were on the order of 60–80 mg/1.25 L. The protein was determined to be >98% pure by SDS-PAGE analysis. Protein concentration was determined at 280 nm using an extinction coefficient of 0.93.[25] Ca^{2+}-free NMR samples of the isolated protein were prepared by adding EDTA to a final concentration of 0.5 m*M*. Small amounts of 1*M* NaOH were added to reach a pH of 8, and the sample was incubated at 308 K for 2 h. A small amount of protein precipitate was removed through centrifugation. EDTA was removed through exchange into the appropriate NMR buffer to ~99% completion by successive dilution in Centricon-10 tubes (Millipore). Final protein concentrations typically ranged from 0.8 to 1.1 m*M*. HSQC analysis of the protein sample before and after chelation with EDTA showed negligible effects on the amide resonances in Δ+PHS.

The blocked tripeptides Ac-Ala-Asp-Ala-NH_2 and Ac-Ala-Glu-Ala-NH_2 were synthesized by the Johns Hopkins Peptide Synthesizer facility. Their purity and composition were assessed by mass spectrometry. Peptides arrived lyophilized and were dialyzed against ddH_2O before dissolving into the appropriate NMR titration buffer (see later).

Crystallization

Crystals of Δ+PHS were grown using hanging drop vapor-diffusion methods at 277 K from a solution containing 17% (v/v) 2-methyl-2,4-pentanediol (MPD) (Sigma-Aldrich), 2*M* equiv $CaCl_2$, 3*M* equiv thymine 3′,5′-diphosphate (pdTp), and 25 m*M* potassium phosphate buffer, pH 8.0. The protein concentration was 18.8 mg mL^{-1} before 1:1 mixing with the reservoir solution in the hanging drop. Δ+PHS nuclease crystallized in primitive monoclinic space group $P2_1$ with cell parameters a = 31.097 Å, b = 60.651 Å, and c = 36.948 Å with angles $\alpha = \gamma = 90.0^\circ$, $\beta = 94.44^\circ$. Crystals appeared after 7–10 days and were mounted in nylon loops on a copper base (CryoLoops™ and CrystalCap Copper Magnetic™ from Hampton Research). Although suspended in the cryoloops, crystals were soaked sequentially in 20, 25, and 30% MPD for 2 min per condition. Immediately after soaking, crystals were flash cooled in liquid nitrogen and stored at 78 K until data collection.

X-ray data collection and structure determination

Diffraction data in the resolution range 31.0–1.8 Å were collected from a single crystal at 110 K using a BRUKER APEX-II diffractometer with CCD detector (Bruker AXS). Data were indexed, integrated, and scaled using SAINT[26] to yield a data set with 14,206 unique reflections. The R_{sigma} value for the data was 0.021 (0.146 in the 1.90–1.80 Å resolution shell); the data were 99.4% complete (99.9% in the 1.90–1.80 Å resolution shell). Using the atomic coordinates for Δ+PHS I92E nuclease determined previously at 277 K as a search model (PDB

accession code 1tqo[27]), a unique rotation and translation solution were generated for the data set by maximum likelihood-based molecular replacement using Phaser[28] software within the CCP4 suite.[29] Rigid body and positional refinement yielded unambiguous electron density maps to 1.8 Å resolution. Structure refinement using Refmac5[30] combined with several cycles of manual model building using Coot[31] resulted in a final overall R_{factor} of 0.196 (0.270 for the 1.85–1.80 Å resolution shell) and an R_{free} of 0.251 (0.362 for the 1.85–1.80 Å resolution shell). Root-mean-square (RMS) deviations of the protein model from ideal geometry calculated by PROCHECK[32] were 0.02 Å for bonds, 1.8° for bond angles, and 5.9° for dihedral angles. One pdTp molecule, one calcium ion, and 106 water molecules were built into the model, which includes protein residues 7–141. Only water molecules with both $2F_o$-F_c and F_o-F_c electron density (contoured at 1.3 σ and 3.0 σ, respectively) and proximity to a likely hydrogen-bond partner (distance < 3.5 Å) were incorporated.

NMR temperature calibration and referencing

Temperature calibration was performed using a 10 m*M* DSS (2,2-dimethyl-2-silapentane-5-sulfonate, Cambridge Isotope Laboratories) sample in 98% D_2O (v/v) over a temperature range of 283–318 K. The chemical shift of the HDO peak was referenced against DSS, which is known to be insensitive to changes in pH and temperature.[33] The NMR set temperature was calibrated by comparing the observed temperature dependence of the HDO chemical shift against its known temperature dependence.

All NMR experiments were referenced against the position of the HDO peak, which was determined relative to the DSS peak in a sample consisting of only NMR buffer (see later) and 1 m*M* DSS. Peaks in the ^{13}C and ^{15}N dimensions were referenced indirectly to the DSS peak.[33] As titration experiments were performed under conditions of different salt concentration and temperature, it was essential to measure the salt dependence of the HDO frequency with respect to DSS. The chemical shift of the HDO peak was measured in six samples of 0.5 m*M* DSS in 98% D_2O or 90% H_2O with salt concentrations ranging between 0 and 1.5*M* KCl at two different temperatures, 298 and 308 K. The salt dependence of HDO with respect to DSS was −9 ppb/0.1*M* salt at 298 K, in accord with the previously measured data.[33] It was −8 ppb/0.1*M* salt at 308 K.

Assignment of NMR spectra

A complete set of H^N, N, Cα, and Cβ assignments for 139/143 residues were obtained at low (pH 4.67) and neutral pH (pH 6.80) using standard HNCACB[34] and CBCA(CO)NH[35] triple-resonance NMR experiments collected at 298 K on a Varian Inova 600 equipped with a cryoprobe (see Supporting Information and BMRB accession number 15901). Complete side chain proton and carbon assignments were collected for all 20 Asp and Glu residues at pH 4.67. Aliphatic side chain ^1H and ^{13}C assignments for Asp and Glu residues except Glu-10 were collected using C—C TOCSY (CO)NH, H—H TOCSY (CO)NH, and HBHA(CO)NH experiments.[36,37] Because Glu-10 immediately precedes a proline residue, side chain chemical shifts were determined with the C—C TOCSY CANH and H—H TOCSY CANH experiments, which correlate aliphatic ^1H or ^{13}C side chain atoms with the H^N of the same residue. These were performed on a Varian Inova 500. Side chain carboxyl carbon (Cγ for Asp, Cδ for Glu) assignments were collected with a three-dimensional version of the HBHGCBCGCO pH titration experiment[38] on a Bruker Avance II-600 equipped with a cryoprobe. All spectra were processed using NMRPipe[39] and analyzed with Sparky.[40]

For low pH assignments, a 1 m*M* solution of Δ+PHS was prepared in a buffer consisting of 25 m*M* potassium acetate, 0.1*M* KCl, 0.5 m*M* NaN_3, and 10% D_2O (v/v). The buffer pH was 4.67, and the final pH of the NMR solution was 4.63–4.66. For neutral pH assignments, a 1 m*M* solution of Δ+PHS was prepared in a buffer consisting of 25 m*M* potassium phosphate, 0.1*M* KCl, 0.5 m*M* NaN_3, and 10% D_2O. The buffer pH was 6.79, and the final pH of the NMR solution was 6.79–6.80. A total of 0.3 mL of each sample was placed in 5-mm tubes (Shigemi).

pH titration experiments

A 1.4-mL sample of 1 m*M* (0.8–1.1 m*M*) protein or 50 m*M* peptide was prepared as described earlier in a buffer of 0.1*M* KCl (or 1.0*M* KCl), 0.5 m*M* NaN_3, and 10% D_2O. This sample was split into two equal fractions, one for titration with acid and the other for titration with base. The initial pH of the protein sample was around pH 5 at the start of the titration experiment; it was pH 2 for model compounds. For each pH increment, the NMR sample was transferred into an Eppendorf tube and mixed with a small volume (μL) of 1*N* HCl (0.1*N* for model compounds) or NaOH (Fisher Scientific), and returned to the NMR tube. The pH was measured in the NMR tube by using a combination pH electrode (Mettler Toledo, Columbus, OH) and an Orion 720A+ pH meter. Readings were taken immediately before and after data acquisition, with the latter value being reported for each spectrum. Variations in pH were 0.05 units or less at pH 7 or lower, and less than 0.10 units between pH 7 and 9, because of the lack of buffering capacity in this pH range. The reported pH values were not corrected for deuterium isotope effects. We estimate a contribution of 25 m*M* salt to the solution from titration with acid and base.

Two-dimensional CBCA(CON)H spectra were collected in 0.5 pH increments between pH 2.5 and 7.5 at 0.1*M* salt and 298 K. Spectra at pH 4.6 and pH 6.9 were assigned based on the previously acquired three-dimensional CBCA(CO)NH spectra. An additional three-dimensional CBCA(CO)NH experiment at pH 3.14 was collected to aid with ambiguous assignments at low pH. The H^N and CBCA planes were zero-filled to 4096 and 1024 points, respectively. Peaks for 130 residues were assigned. The total acquisition time for each pH increment was ~2.5 h.

$^1H^N$ and ^{15}N backbone amide chemical shifts at 0.1 and 1*M* KCl were measured as a function of pH by collecting a series of [^{15}N—^1H]-HSQC[41] spectra in 0.4 pH increments between pH 2 and 9. The ^{15}N carrier frequency was set to 117.9 ppm. A total of 100 complex t_1 experiments were collected with four transients using a spectral width of 2008 Hz in the ^{15}N dimension. The data were zero-filled to 4096 and 1024 points in the ^1H and ^{15}N dimensions, respectively. The total acquisition time for each HSQC spectrum was ~20 min.

The chemical shifts of the Asp and Glu carboxyl side chain carbons and their adjacent methylene protons were monitored as a function of pH with modified two-dimensional versions of the HBHG(CBCG)CO experiment.[38] In this experiment, Asn and Gln signals were removed by evolving these as multiple-quantum coherences, which are rendered undetectable, whereas the carboxyl side chain carbons of Asp and Glu residues remained unaffected. The ^{13}C carrier frequency was set to ~180.6 ppm, the center of the carboxyl carbon region. In the ^{13}C dimension, a total of 52 complex t_1 experiments were collected with 32 transients and a spectral width of 1510 Hz. The total acquisition time for each pH increment was ~2 h. Linear prediction of 10 complex points was applied to the ^{13}C dimension. The t_2 and t_1 dimensions were zero-filled to 4096 and 1024 points, which yielded a digital resolution of 2.4 and 1.5 Hz/pt in the ^1H and ^{13}C dimensions, respectively. Glu-73 and Glu-75 carboxyl side chain carbon resonances were not observed in the HBHG(CBCG)CO spectra collected at 298 K. The sensitivity of these signals was enhanced when the temperature was raised to 308 K. At this temperature and below pH 3, a significant amount of protein precipitated, especially in 1*M* KCl. For this reason, a ^{13}C-detect version of the HBHG(CBCG)CO experiment was designed to circumvent the sensitivity issues experienced with Glu-73 and Glu-75 at 298 K (Castañeda and Majumdar, unpublished).

Analysis of titration curves

Nonlinear least squares analysis with the nlme library in the *R* statistics package[42] was used to determine the pK_a values. The modified Hill equation[43] was fitted to the pH dependence of the side chain carboxyl carbon chemical shifts:

$$\delta_{obs}(pH) = \frac{\delta_{AH} + \delta_{A-} \cdot 10^{n\cdot(pH-pK_a)}}{1 + 10^{n\cdot(pH-pK_a)}} \quad (1)$$

In this expression, δ_{AH} and δ_{A-} are the chemical shifts for the protonated and deprotonated species of the carboxylic residue. The Hill coefficient, *n*, represents the slope of the titration curve in the transition region. The pK_a value represents the pH at which the ionizable group is protonated halfway. In cases where a second titration event was apparent, the fit was performed with a two-site binding isotherm[44]:

$$\delta_{obs}(pH) = \frac{\delta_{AH2} + \delta_{AH} \cdot 10^{(pH-pK_{a1})} + \delta_{A-} \cdot 10^{(2\cdot pH-pK_{a1}-pK_{a2})}}{1 + 10^{(pH-pK_{a1})} + 10^{(2\cdot pH-pK_{a1}-pK_{a2})}} \quad (2)$$

The two pK_a values, pK_{a1} and pK_{a2}, represent each titration event. Note that there is no Hill coefficient in the two-site binding isotherm so that the number of fitting parameters is minimized.

Several Cγ and Cδ titrations for Asp and Glu residues (Asp-19, Asp-95, Glu-10) were incomplete in the acid limit (Table II and Fig. 3). These same residues exhibited full titration curves at 1*M* salt. In these cases, the amplitude (Δδ) of the titration at 0.1*M* salt was fixed to the value determined from the fit at 1*M* salt. This is justified because Asp and Glu residues with complete titration curves under both 0.1 and 1*M* salt have nearly identical Δδ parameters.

The resonances of Glu-75 were broadened beyond detection below pH 4 at 1*M* salt; however, a partial titration of Glu-75 was still observed. The origins of the weak resonances of Glu-75 (see Fig. 2) are not understood at this time. The amplitude (Δδ) of the Cδ titration was fixed at either 3 or 4 ppm, which are typical values observed for Asp and Glu residues in proteins. This bracketed the pK_a value of Glu-75 to be between 3.91 and 4.16 at 1*M* salt.

Continuum electrostatics calculations

Calculations were performed with the structures of the wild-type SNase[45] (PDB accession code 1stn), Δ+PHS (PDB accession code 3bdc), and with a model of Δ+PHS made from the structure of the Δ+PHS/V66K variant[23] described previously.

pK_a values and H^+ titration curves were calculated with the method based on the FDPB equation using the University of Houston Brownian Dynamics package,[12,46–48] as discussed previously for SNase.[17,49] Hydrogen atoms were added to the molecular structure using the HBUILD utility of CHARMm[50] version 25.3. The positions of hydrogen atoms were energy minimized

with 500 steps of steepest descent minimization performed with all heavy atoms kept static. The default placement of hydrogen atoms was on Oδ2 for all Asp residues and Oε2 for all Glu residues, unless noted otherwise. Calculations were performed at 298 K and 0.10 or 1.0*M* ionic strength. The solvent dielectric constant was set to 78.5, and the protein interior was treated with a dielectric constant (ε_{in}) of 20 or 78.5. The charge state of the protein and the pK_a values were calculated using the cluster method of Gilson[51] based on the thermodynamic cycle of Warshel.[52] Both single-site[47,48] and full-site[12,53] charging schemes were used.

RESULTS

Crystal structure of Δ+PHS nuclease

Wild-type SNase unfolds in the range of pH where carboxylic groups titrate.[18] Therefore, to measure the pK_a values, it was necessary to use a hyperstable variant of SNase known as Δ+PHS, which remains folded under relatively acidic conditions. This variant includes a truncation (residues 44–49) and five substitutions (G50F, V51N, P117G, H124L, and S128A). To describe the microenvironments of the acidic groups and to show that the variant is comparable to the wild type, the crystal structure of Δ+PHS was determined. Crystallographic statistics are listed in Table I. The overall and Cα RMSD between Δ+PHS and the wild type (PDB accession code 1snc) were less than 0.4 and 0.2 Å, respectively.

SNase has 21 carboxylic groups: eight Asp, 12 Glu, and the C-terminal COOH (see Fig. 1). Four of these groups (Glu-142, Asp-143, Asp-146, and the C-terminal COOH) are invisible in this and in all other crystal structures of SNase. Seven of the carboxylic groups are in α-helices, two are in β-strands. The remaining six Asp and two Glu residues are in turns, loops, and other less-structured regions of the protein. Five carboxylic groups (Asp-19, Asp-21, Asp-40, Glu-43, and Glu-52) are clustered in the active site region.

Table I
X-Ray Refinement Statistics for Δ+PHS

PDB accession code	3bdc
Temperature (K)	110
pH	8
Space group	$P2_1$
Unit cell parameters	a = 31.10 Å
	b = 60.65 Å
	c = 36.95 Å
	β = 94.44°
Wavelength (Å)	1.5418
Resolution range (Å)	31.0–1.8 (1.9–1.8)
Number of unique reflections	14,206 (1901)
Redundancy	13.18 (7.86)
Completeness (%)	99.4 (100.0)
Mean I/s	51.9 (6.2)
R_{sigma}	0.021 (0.146)
Wilson B-factor (Å^2)	28.1
Resolution range (Å)	31.01–1.80 (1.85–1.80)
Number of reflections	10,735 (737)
Nonhydrogen protein atoms	1047
Waters	106
Ligand atoms	25
Ions	1
R (90% of data)	0.196 (0.270)
R_{free} (10% of data)	0.251 (0.362)
RMSD for ideal geometry	
Bond length length (Å)	0.02
Bond angle (°)	1.8
Dihedral angle (°)	5.9
Average B-factors (Å^2)	
Protein atoms	21.3
Waters	27.6
Ligand atoms	18.4
Ions	23
Ramachandran plot	
Most favored regions (%)	101 (88.6)
Additionally allowed regions (%)	12 (10.5)
Generously allowed regions (%)	0 (0.0)
Disallowed regions (%)	1 (0.8)

pK_a values of Asp and Glu residues

A reference set of pK_a values was obtained by monitoring the pH dependence of the Cγ or Cδ chemical shift of the Asp and Glu side chains in blocked peptides (Ac-ADA-NH_2, Ac-AEA-NH_2) in 0.01, 0.1, and 1.0*M* KCl at 298 K. The pK_a values of Asp and Glu in these peptides were 3.90 ± 0.01 and 4.35 ± 0.01, respectively (Table II), and they were insensitive to KCl concentrations between 0.01 and 1.0*M* KCl. These pK_a values are consistent with values of 3.9 ± 0.1 and 4.2 ± 0.1 measured with NMR spectroscopy for Asp and Glu, respectively.[54–56]

Full backbone and side chain assignments for Asp and Glu residues in SNase were completed at pH 4.67 (Supporting Information). The pK_a values of Asp and Glu residues in SNase were measured by monitoring the pH dependence of the chemical shifts of Cγ or Cδ with two-dimensional HBHG(CBCG)CO experiments.[38] A typical HBHG(CBCG)CO spectrum is shown in Figure 2. pH titrations of the Cγ or Cδ chemical shift of each carboxylic group at 0.1 and 1*M* KCl are shown in Figure 3. The pK_a values of Asp and Glu residues obtained by fitting a modified Hill equation or a two-site binding isotherm [Eqs. (1) and (2)] to the data in Figure 3 are listed in Table II. The pK_a values for the incomplete titration curves of Asp-19, Asp-95, and Glu-10 at 0.1*M* salt were obtained by fixing the Δδ parameter to the value obtained from the titration curves at 1*M* salt, as described in detail in Materials and Methods. Plots of the titration curve of side chain Hβ/Hγ resonances and the pK_a values determined from them are provided in Supporting Information.

With the exception of Asp-21, the pK_a values of all carboxylic groups were depressed relative to the values

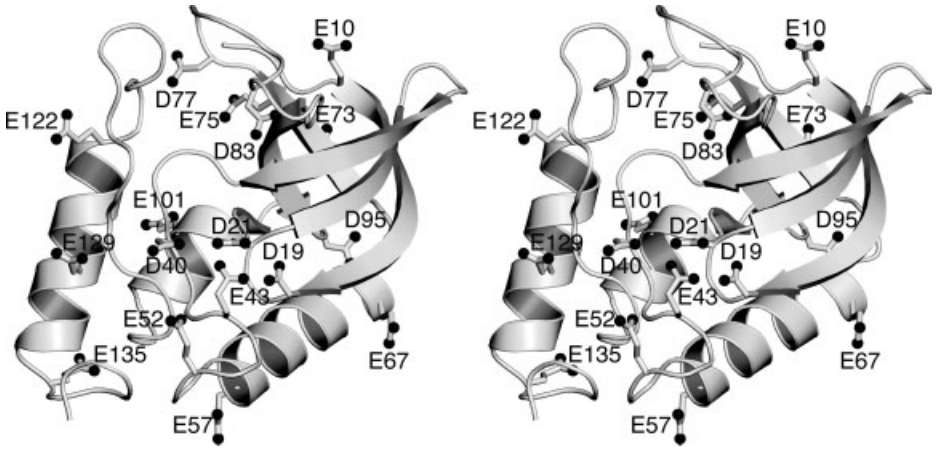

Figure 1

Stereo view of Δ+PHS SNase showing all Asp and Glu residues; Oδ (Asp) and Oε (Glu) atoms are represented as black spheres. Three residues (Glu-142, Asp-143, and Asp-146) are not visible in the crystal structure. (PDB accession code: 3bdc).

measured in model peptides. In 0.1*M* salt, three Asp residues (Asp-40, Asp-143, and Asp-146) and 11 Glu residues (Glu-43, Glu-52, Glu-57, Glu-67, Glu-73, Glu-75, Glu-101, Glu-122, Glu-129, Glu-135, and Glu-142) titrated with pK_a values within 1.1 units of their respective normal values. Only six residues (Glu-10, Asp-19, Asp-21, Asp-77, Asp-83, and Asp-95) experienced large pK_a shifts $\geq$1.5 units. These six residues are all located in irregular structures, loops, or turns in the protein (see Fig. 1). The Hill coefficients obtained from the fits ranged from 0.57 to 0.99 with an average of 0.79 $\pm$ 0.11.

Four of the six residues that titrated with large pK_a shifts (Asp-19, Asp-21, Asp-77, and Asp-83) exhibited unusual behavior. For example, in 0.1*M* salt, neither Asp-77 nor Asp-83 titrated between pH 2 and 9. This could mean that the pK_a values of these residues are either below 2 or above 9. If the pK_a values were elevated, the stability ($\Delta G^{\circ}_{H_2O}$) curve of this protein would exhibit a significant pH dependence, which it does not.[23,57] Furthermore, in 1*M* salt, there were slight indications that both of these groups begin to titrate at low pH (see Fig. 3). For these reasons, the pK_a values were assigned an upper bound of 2.2, which corresponds to the pH at the midpoint of the global acid unfolding for this protein as monitored by far-UV circular dichroism and Trp fluorescence.[57] The other two groups with unusual behavior, Asp-19 and Asp-21, had to be treated with two-site binding isotherms because the ionization of a second carboxylic group was evident in the shape of the titration curve [Eq. (2)]. In these cases, the transition with the largest amplitude was the one used to obtain the pK_a of the residue. Asp-19 titrated with a pK_a of 2.21; the amplitude of its titration was very small (1.8 ppm) compared with the titration curves of other Asp and Glu residues (3–4 ppm).[5] Asp-21 titrated with a pK_a of 6.54. This is the only carboxylic residue in SNase with an elevated pK_a relative to the normal value. The shift of 2.6 pK_a units at 0.1*M* salt is also the largest shift of any carboxylic group in SNase.

The resonances of Glu-73, Glu-75, and Asp-77 were significantly weaker than the resonances of the other Asp and Glu residues in the protein. These residues were affected by severe methylene proton relaxation or exchange broadening effects for unknown reasons. Additionally, the resonance of Asp-21 broadened significantly

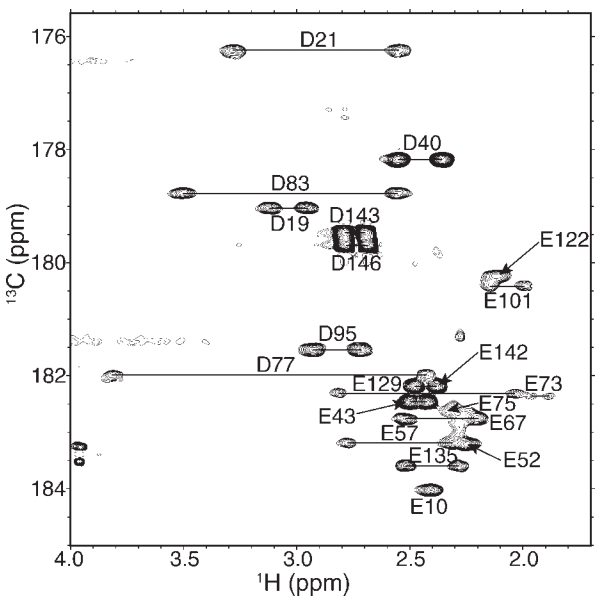

Figure 2

Sample HBHG (CBCG) CO spectrum of Δ+PHS (1 m*M* protein, 308 K, 0.1*M* KCl, pH 4.65) showing only Hβ-Cγ and Hγ-Cδ side chain connectivities for Asp and Glu residues, respectively. Assignments for all 20 Asp and Glu residues are shown.

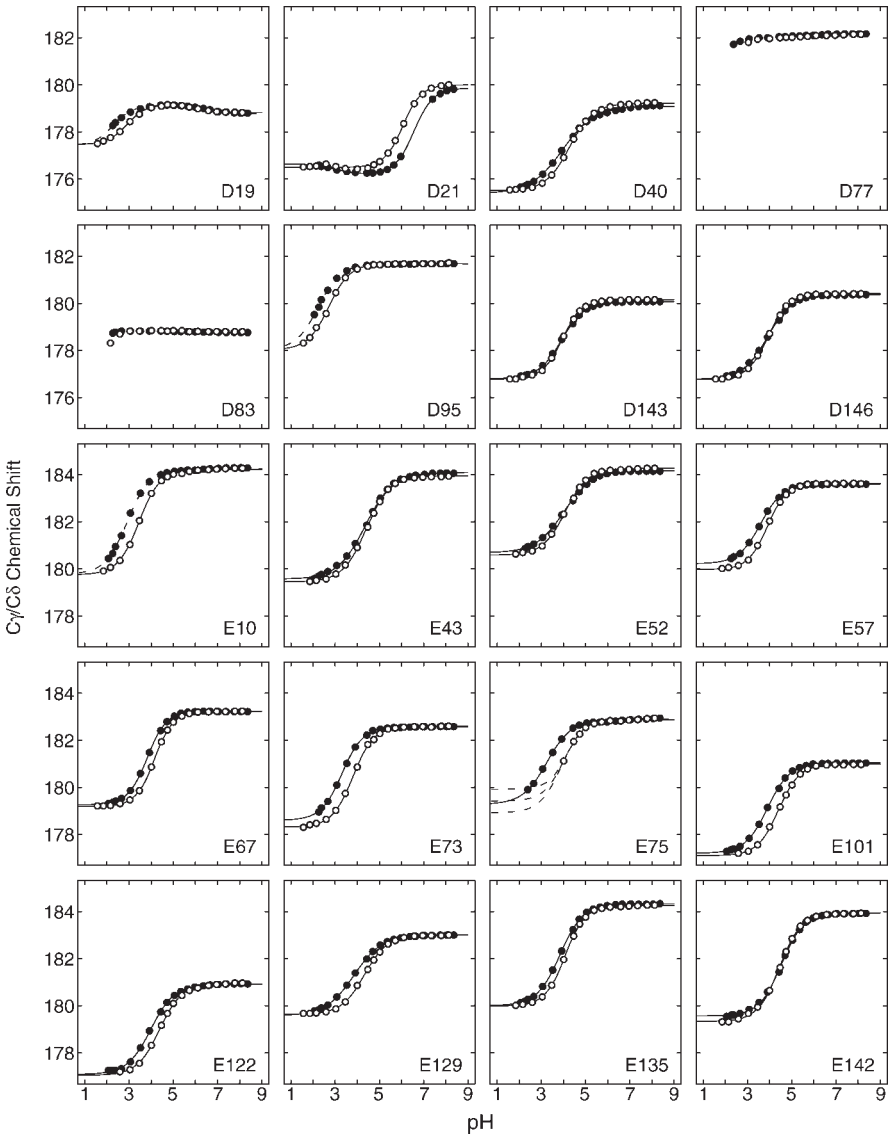

Figure 3

Titration curves for carboxylic residues in Δ+PHS at 0.1*M* (●) and 1.0*M* (○) KCl and 298 K as observed by monitoring the chemical shift of Cγ/Cδ resonances.

near its pK_a value. No other residue exhibited this behavior.

Methylene protons (Hβ/Hγ) of carboxylic groups are notoriously unreliable reporters of pK_a values because they are susceptible to influences from nearby titrating carboxylic groups and from pH-dependent conformational changes in the protein.[58,59] Despite these shortcomings, the pH dependence of Hβ/Hγ resonances can provide a useful comparison and supplement the pK_a values of carboxylic groups obtained by monitoring Cγ and Cδ chemical shifts. The pK_a values obtained from Hβ and Hγ resonances (listed in Supporting Information) were not as well determined as the pK_a values in Table II, but they were all within 0.5 units.

Salt sensitivity of pK_a values

To examine the magnitude of contributions from Coulomb interactions, the pK_a values were measured in 0.1 and 1*M* KCl. In contrast to the marked salt sensitivity of the pK_a value of His residues in model compounds in water,[60] the pK_a values of Asp and Glu residues in model compounds were insensitive to salt in the range 0.01–1*M*. Four groups in SNase (Glu-43, Glu-142, Asp-143, and

Table II
pK_a Values of Asp and Glu Residues in SNase

	0.1*M* KCl			1.0*M* KCl		
Residue	pK_a[a]	ΔpK_a[b]	n[a]	pK_a[c]	ΔpK_a[b]	n[c]
Asp[d]	3.90 ± 0.01[c]	–	1.01 ± 0.02[c]	3.90 ± 0.02	–	0.97 ± 0.03
Asp-19	2.21 ± 0.07, 6.54 ± 0.06[e]	−1.69	–	2.92 ± 0.02, 6.08 ± 0.11	−0.98	
Asp-21	3.01 ± 0.01, 6.54 ± 0.02	2.64	–	6.06 ± 0.03	2.16	1.04 ± 0.05
Asp-40	3.87 ± 0.09	−0.03	0.57 ± 0.02	4.28 ± 0.01	0.38	0.81 ± 0.01
Asp-77	<2.2	<−1.7	–	<2.2	<−1.7	–
Asp-83	<2.2	<−1.7	–	<2.2	<−1.7	–
Asp-95	2.16 ± 0.07[e]	−1.74	0.87 ± 0.02[e]	2.71 ± 0.02	−1.19	0.90 ± 0.03
Asp-143	3.80 ± 0.10	−0.10	0.77 ± 0.04	3.94 ± 0.01	0.04	0.96 ± 0.01
Asp-146	3.86 ± 0.05	−0.04	0.75 ± 0.01	3.93 ± 0.01	0.03	0.92 ± 0.01
Glu[d]	4.36 ± 0.01[c]	–	0.98 ± 0.01[c]	4.35 ± 0.01	–	1.00 ± 0.01
Glu-10	2.82 ± 0.09[e]	−1.53	0.85 ± 0.02[e]	3.45 ± 0.02	−0.90	0.91 ± 0.03
Glu-43	4.32 ± 0.04	−0.03	0.69 ± 0.01	4.40 ± 0.01	0.05	0.81 ± 0.02
Glu-52	3.93 ± 0.08	−0.42	0.65 ± 0.03	4.08 ± 0.02	−0.27	0.84 ± 0.02
Glu-57	3.49 ± 0.09	−0.86	0.83 ± 0.03	3.90 ± 0.01	−0.45	0.98 ± 0.02
Glu-67	3.76 ± 0.07	−0.59	0.99 ± 0.03	4.16 ± 0.00	−0.19	1.03 ± 0.01
Glu-73	3.31 ± 0.01[c]	−1.04	0.92 ± 0.01[c]	3.80 ± 0.01	−0.55	0.91 ± 0.02
Glu-75	3.26 ± 0.05[c]	−1.09	0.79 ± 0.04[c]	(3.91−4.16)[f]	∼−0.3	(0.89–1.03)[f]
Glu-101	3.81 ± 0.10	−0.54	0.82 ± 0.02	4.41 ± 0.01	0.06	0.91 ± 0.02
Glu-122	3.89 ± 0.09	−0.46	0.78 ± 0.03	4.38 ± 0.02	0.03	0.86 ± 0.03
Glu-129	3.75 ± 0.09	−0.60	0.66 ± 0.03	4.32 ± 0.01	−0.03	0.83 ± 0.01
Glu-135	3.76 ± 0.08	−0.59	0.82 ± 0.01	4.08 ± 0.01	−0.27	0.95 ± 0.01
Glu-142	4.49 ± 0.04	0.14	0.85 ± 0.01	4.45 ± 0.01	0.10	0.88 ± 0.02

[a] pK_a values of carboxylic groups measured at 298 K by monitoring the Cγ/Cδ resonances of Asp/Glu residues. The pK_a values and Hill coefficients (n) were extracted from fitting Eq. (1) or (2) to the experimental titration curve. No Hill coefficients were extracted when a two-site model was used for the fit [Eq. (2)]. In cases where the two-site model was used, the pK_a of the major transition is underlined. The means and standard deviations of pK_a values and Hill coefficients over three independent titration experiments are reported here, unless otherwise indicated. The standard deviations include experimental error from variability in protein batch, pH electrode, and protein solution preparation.
[b] pK_a shifts relative to model compound values in water: $\Delta pK_a = pK_a - pK_a^{mod}$, where pK_a^{mod} is 3.90 for Asp and 4.35 for Glu at both 0.1 and 1*M* salt.
[c] pK_a values and Hill coefficients with fitting errors from a single titration experiment.
[d] pK_a of carboxylic group measured at 298 K by monitoring the Asp Cγ or Glu Cδ resonance in the model compound Ac-Ala-X-Ala-NH_2, where X is Asp or Glu.
[e] pK_a and Hill coefficient determined by fixing the amplitude (Δδ) of the titration to the Δδ obtained from the fit at 1*M* KCl.
[f] Range of pK_a values and Hill coefficients determined by fixing the amplitude (Δδ) of the Glu-75 Cδ titration between 3 and 4 ppm, which are typical values observed for Glu Cδ titrations in proteins.

Asp-146) with nearly normal pK_a values were similarly salt insensitive, whereas the pK_a values of the remaining carboxylic groups shifted by ∼0.5 units toward model compound pK_a values when salt concentration was increased from 0.1 to 1*M*.

In 1*M* salt, the pK_a values of 14 carboxylic groups titrated within 0.5 units of their model compound values (Table II). The six residues (Asp-19, Asp-21, Asp-77, Asp-83, Asp-95, and Glu-10) with the most shifted pK_a values in 0.1*M* salt also had pK_a values shifted by >1 unit relative to model compound values at 1*M* salt. Asp-21 titrated with a highly perturbed pK_a (shifted by 2.16 units) even in 1*M* salt. Under these conditions, Asp-40 also titrated with a slightly elevated pK_a, shifted by 0.38 units relative to model compound values.

The carboxylic groups in the active site of SNase are known to bind Ca^{2+}. Indeed, a site-bound Ca^{2+} ion is observed in the crystal structure of Δ+PHS nuclease. To examine the potential influence of traces of Ca^{2+} on the pK_a values of carboxylic groups, pK_a values were also measured in samples treated extensively with EDTA to remove Ca^{2+} from solution. The pK_a values thus measured were found to be indistinguishable from the values measured in samples without EDTA, which presumably have traces of Ca^{2+}.

Structural reorganization coupled to changes in pH

To identify evidence for structural reorganization coupled to a change in pH above the acid-unfolding transition at pH 2.2, the pH dependence of H^N, Cα, and Cβ resonances was measured for each residue between pH 2.5 and 8.0. The amplitudes of the pH-dependent changes are shown in Figure 4. In this figure, upfield shifts with decreasing pH are positive, downfield shifts are negative. The different types of resonances report on different aspects of the structure. The pH dependence of H^N chemical shifts has been used previously to show that the overall structure of the backbone was unaffected during the course of a pH titration.[61] Furthermore, the H^N resonances that are hydrogen bonded to carboxylic groups exhibit large pH-dependent changes and titrations mirroring those of the carboxylic groups to which they are hydrogen bonded. In contrast, the Cα chemical shift

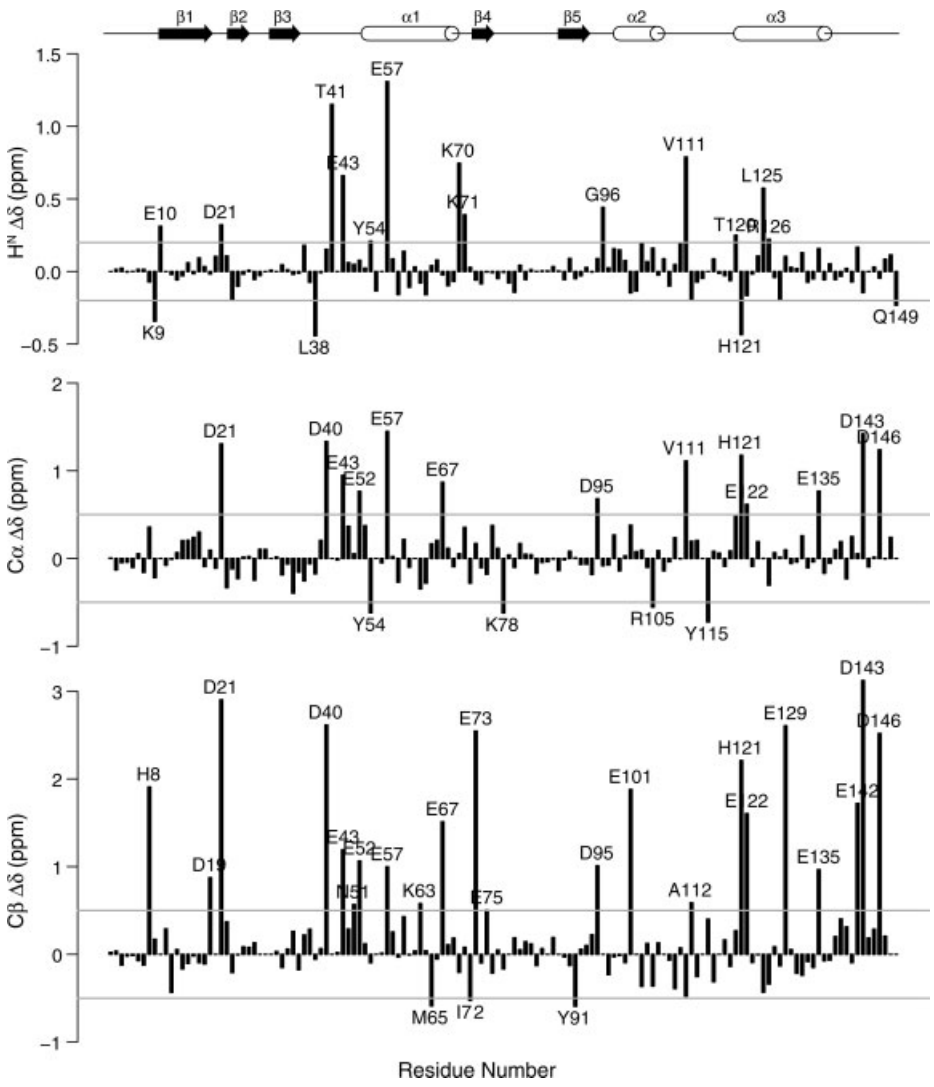

Figure 4

pH dependence of the H^N, Cα, and Cβ chemical shifts in Δ+PHS collected at 0.1*M* KCl and 298 K. H^N Δδ = δ(pH ~8.5) − δ(pH ~2). Cα Δδ and Cβ Δδ = δ(pH ~7.5) − δ(pH ~2.5). Those resonances with larger pH-dependent shifts than 0.2 ppm (H^N) or 0.5 ppm (Cα and Cβ) are labeled. Gray lines indicate these cutoffs.

can probe changes in secondary structure.[62] Both Cα and Cβ resonances report on the titration of side chain carboxylic groups, although the effects of the titration elicit pH-dependent changes smaller than those of side chain Cγ or Cδ atoms.[63]

The data show that the overall secondary and tertiary structure of SNase remained unchanged between pH 8.0 and 2.5. Of the 137 observable H^N resonances, only 17 showed pH-dependent changes larger than 0.2 ppm between pH 2 and 8.5. These resonances are labeled in Figure 4. Nine of these 17 H^N resonances (Asp-21, Thr-41, Glu-43, Tyr-54, Glu-57, Lys-70, Lys-71, Gly-96, and Val-111) are hydrogen bonded to Asp and Glu residues; they are reporting on the titration of their hydrogen-bonding partner. The H^N resonances of Lys-9 and Gln-149 exhibited pH-dependent changes that reported on the titration of His-8 and the C-terminus carboxylic group, respectively. Of the 137 Cα and 137 Cβ signals, only 17 Cα and 25 Cβ resonances showed pH-dependent changes larger than 0.5 ppm between pH 2.5 and 7.5 (see Fig. 4). Of these 42 resonances, 31 reported on the titrations of Asp, Glu, and His residues. These resonances titrated with pK_a values that matched the pK_a values of their side chain ionizable group in Table II (data not shown). Only 16 Cα, Cβ, and H^N resonances exhibited pH-dependent changes that could not be easily explained in terms of titration of a neighboring Asp or Glu residue.

DISCUSSION

To examine molecular determinants of the measured pK_a values, the microenvironments of the carboxylic group in 10 crystal structures of SNase, including the structure of Δ+PHS SNase, were analyzed (Table I in Supporting Information). The Cα RMSD among these 10 structures is 0.27 Å ± 0.09. Only the backbone of residues 113–117 and the side chains of Asp-40 and Glu-43 were in different conformations in the different structures, depending on the presence or absence of a ligand at the active site. Except for the carboxylic groups in the active site (Asp-19, Asp-21, Asp-40, Glu-43) and Glu-101, the conformations of the carboxylic side chains in the different structures were indistinguishable. The microenvironment of Glu-101 is different between the structures of wild-type SNase and Δ+PHS because a potential hydrogen bond with Ser-128 is eliminated when the residue is substituted with Ala in Δ+PHS. Solvent accessibility calculations using NACCESS[64] suggest that the carboxylic groups are fully solvent-exposed with the exceptions of Asp-77 and Asp-83; their oxygen atoms are less than 10% accessible.

Table III
Hydrogen Bonds of Carboxylic Groups in SNase

	0.1*M* KCl		1.0*M* KCl	
Hydrogen bond[a]	H^N Δδ (ppm)[b]	H^N pH_{mid}[c]	H^N Δδ (ppm)	H^N pH_{mid}
Asp-21 H^N—Asp-19	>0.3	<2.2[d]	0.59	2.83 ± 0.03
Thr-41 H^N—Asp-21	1.15	6.42 ± 0.01	1.06	5.95 ± 0.03
Lys-70 H^N—Asp-95	~1	<2.2[e]	~1	2.76 ± 0.01[e]
Lys-71 H^N—Asp-95	~1	<2.2[e]	~1	2.88 ± 0.01[e]
Glu-43 H^N—Glu-52	0.77	3.78 ± 0.09	0.83	3.96 ± 0.04
Tyr-54 H^N—Glu-57	0.23	3.23 ± 0.03	0.25	3.69 ± 0.11
Glu-57 H^N—Glu-57	1.38	3.43 ± 0.02	1.48	3.81 ± 0.02
Gly-96 H^N—Glu-73	0.49	3.36 ± 0.03	0.46	4.08 ± 0.03
Val-111 H^N—Glu-129	0.85	3.81 ± 0.04	0.99	4.22 ± 0.03

[a]Hydrogen bonds between the amide protons and the side chains of carboxylic groups were identified as cases where the pH_{mid} of the H^N titration matched the pK_a of the nearby carboxylic group detected through the crystal structure analysis (Table I in Supporting Information). Data were collected at either 0.1*M* KCl and 298 K or 1.0*M* KCl and 308 K. Titration curves are supplied in Supporting Information.
[b]The amplitude ($\delta_{A-} - \delta_{AH}$) of the transition associated with titration of the nearby carboxylic group.
[c]The pH_{mid} is the apparent pK_a reported from fitting the titration curve to Eq. (1) or (2).
[d]pK_a determined by fixing the amplitude (Δδ) of the titration to Δδ obtained from the fit at 1*M* KCl.
[e]pK_a determined by fixing the amplitude (Δδ) of the titration between 1.0 and 1.5 ppm.

Hydrogen bonding

Hydrogen bonds are known to depress the pK_a of Asp or Glu residues.[5,8,14,22,65,66] The effect can range from ~0.5 to 1.5 pK_a units. Hydrogen bonds between Asp and Glu residues and backbone amide protons (H^N) can be identified with NMR spectroscopy by correlating the pH dependence of backbone H^N resonances with the titrations of Asp and Glu residues.[56,67,68] A H^N resonance that shifts upfield by >0.2 ppm[68] with decreasing pH (positive Δδ in Fig. 4) and has a pH_{mid} that matches the pK_a of the nearest carboxylic group (within 0.2 units) is a likely participant in a hydrogen bond with that carboxylic group. Using this criterion, nine hydrogen bonds between the backbone and seven carboxylic residues were identified (Table III).

The putative hydrogen bonds in Table III can be classified into two categories based on the amplitude of the H^N titration (H^N Δδ). No absolute correlation between hydrogen bond strength and H^N Δδ has ever been established.[5,68] Five carboxylic groups (Asp-21, Asp-95, Glu-52, Glu-57, and Glu-129) are in six hydrogen bonds in one category because the H^N resonance exhibited large pH-dependent shifts of >0.8 ppm at both 0.1 and 1*M* salt. These hydrogen bonds are consistently identified in structures of SNase by the hydrogen-bond calculator HB-PLUS[69] [Fig. 5(a) and Table I in Supporting Information]. Interestingly, according to HB-PLUS, Glu-129 is in a strong hydrogen bond with the H^N of Val-111, which should depress its pK_a, yet the pK_a of Glu-129 at 1*M* salt is normal (Table II), consistent with the observation that pK_a values of Glu residues tend not to be as sensitive to hydrogen bonds as those of Asp residues.[5]

The remaining three hydrogen bonds in Table III have H^N Δδ values <0.5 ppm; these are not predicted with HB-PLUS because the N—O pairwise distances are larger than they should be for hydrogen bonds.[69] The hydrogen bond between Glu-73 and the H^N of Gly-96 is a special case; the N—O distance is consistently >5 Å. We hypothesize that a water molecule participates in a hydrogen bond network with these two residues [Fig. 5(a)]. This water molecule is conserved in 69 of 71 crystal structures of SNase examined (data not shown). Ordered crystallographic water molecules have been observed near the carboxyl oxygens of the Asp and Glu residues in many protein structures.[70,71] In this respect, it is also noteworthy that the pK_a of Glu-73 is depressed by 1.0 units at 0.1*M* KCl despite Glu-73 being surrounded primarily by crystallographic water molecules (Table I in Supporting Information).

Hydrogen bonds between carboxylic groups and polar atoms from nearby side chains are not as easy to detect with NMR spectroscopy as hydrogen bonds with the backbone. However, the intramolecular interactions summarized in Table I in Supporting Information and the results from HB-PLUS suggest that five residues (Glu-10, Asp-21, Glu-75, Asp-77, and Glu-135) are in hydrogen bonds with nearby polar side chains, and four (Glu-75, Asp-83, Glu-122, and Glu-135) are in hydrogen bonds with ionizable side chains in at least half of the crystal structures examined. The hydrogen bonds that are found consistently across all structures of SNase are shown in

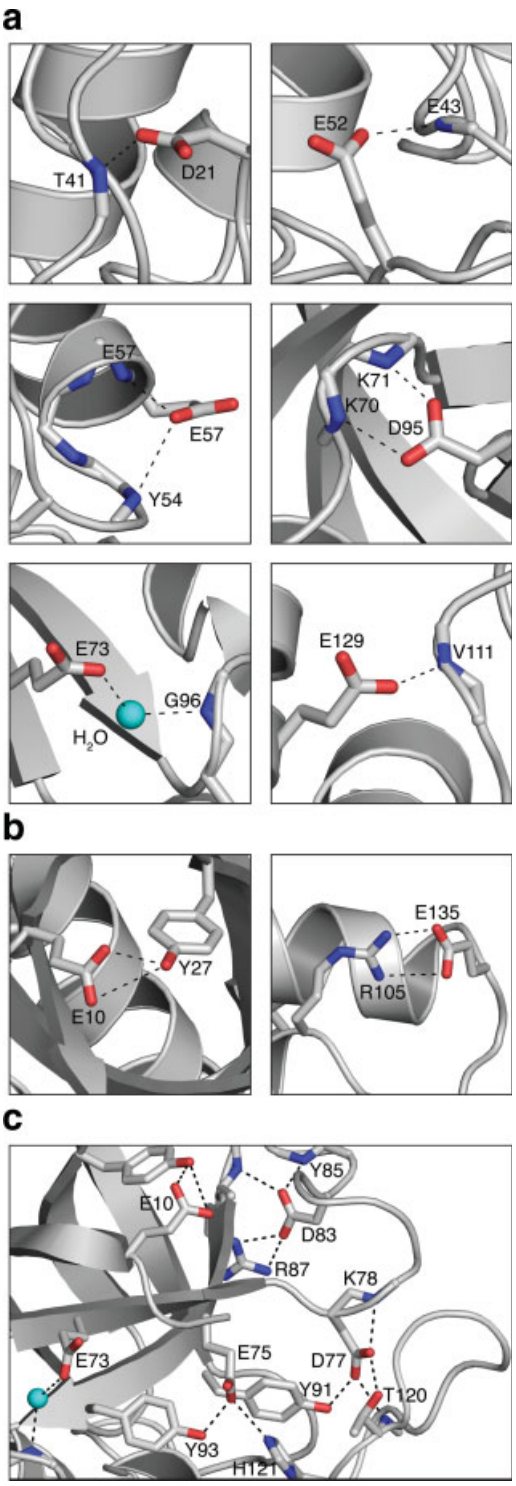

Figure 5

Hydrogen bonds and electrostatic interactions of Asp and Glu residues. (**a**) Hydrogen bonds between carboxylic groups and backbone amide groups that are confirmed by NMR spectroscopy data. (**b**) Side chain hydrogen bonds between Glu-10 and Tyr-27, and the putative electrostatic interaction between Glu-135 and Arg-105. (**c**) The complex hydrogen bonding and electrostatic network involving carboxylic residues Glu-75, Asp-77, and Asp-83. Shown nearby are Glu-10 and Glu-73 and their hydrogen bonding partners.

Figure 5(b,c). No correlation was found between the frequency with which hydrogen bonds are predicted by HB-PLUS and the shifts in the pK_a value of the Asp or Glu residues. However, it should be noted that Asp-77 and Asp-83, which make four hydrogen bonds each [Fig. 5(c)], are also the two groups with the most shifted pK_a values.

Overall, the analysis of crystal structures (Table I in Supporting Information) suggests that 14 of the 20 Asp and Glu residues are involved in at least one hydrogen bond with protein atoms. The correlation between the titrations monitored by H^N atoms with those of the nearby carboxylic group corroborated the hydrogen bonds between carboxylic groups and H^N atoms that were identified by HB-PLUS. The possibility of hydrogen bonding interactions between the backbone atoms of Lys-78, Tyr-85, Arg-87, and Thr-120 and the carboxylic groups of Asp-77 and Asp-83 [Fig. 5(c)] could not be confirmed by NMR because these residues do not titrate in the range of pH that was studied. Notably, the six residues (Glu-10, Asp-19, Asp-21, Asp-77, Asp-83, and Asp-95) that have pK_a values shifted by >1 unit at both 0.1 and 1M salt are involved in hydrogen bonds with near ideal geometry. The stabilizing hydrogen bonds are probably responsible for the large shifts in the pK_a values of these six Asp and Glu residues. The magnitude of these effects is comparable to those described in earlier experimental[5,65,66] and computational[8,14,22] studies.

Coulomb interactions

The pK_a values of Asp and Glu residues in model compounds are salt insensitive; therefore, it is possible to interpret the salt dependence of the pK_a values of carboxylic groups in the protein in terms of screening of Coulomb interactions. The average shift in the pK_a of 14 Asp and Glu residues was 0.49 $\pm$ 0.15 between 0.1 and 1.0M salt, which is greater than the shifts observed previously for the pK_a values of histidines in SNase and myoglobin.[60,72] Increasing salt concentration always increased the pK_a values of carboxylic groups in SNase because salt screens the favorable medium and long-range Coulomb interactions with basic groups that depress pK_a values of the carboxylic groups.

There are significant repulsive electrostatic interactions among some of the carboxylic groups, and these effects are reflected in the Hill coefficients obtained from fitting the modified Hill equation [Eq. (1)] to the titration data. Independent sites titrate with Hill coefficients of 1, as observed with Asp and Glu residues in the model compounds at all salt concentrations. In contrast, the Asp and Glu residues in SNase titrated with Hill coefficients <1. In 0.1M salt, the average Hill coefficient was 0.79 $\pm$ 0.11 and in 1M salt it increased to 0.91 $\pm$ 0.07, consistent with increased screening of interactions between carboxylic groups. Four residues (Asp-40, Glu-43, Glu-52,

and Glu-129) have low Hill coefficients under all conditions studied. Asp-40 exhibited the most shallow titration curve of all carboxylic groups with Hill coefficients of 0.57 and 0.81 at 0.1 and 1*M* salt, respectively (Fig. 3 and Table II). Low Hill coefficients were to be expected for Asp-40, Glu-43, and Glu-52 because they are all part of the cluster of carboxylic groups near the active site (Table I in Supporting Information). The molecular origins of the low Hill coefficient of Glu-129 are less obvious; this residue is at least 8 Å from the nearest carboxylic group in crystal structures of SNase.

In the crystal structures, the majority of Asp and Glu residues are within 6.4 Å of a Lys or Arg residue (Table I in Supporting Information), suggesting that strong, favorable medium to short-range Coulomb interactions are possible. However, the pK_a values of 14 of the 20 carboxylic groups in 1*M* salt were within 0.5 units of their model compound values (Table II). Large *B*-factors of basic residues and large standard deviations in the pairwise distances (Table I in Supporting Information) between carboxylic groups and these residues suggest that flexibility attenuates the strength of these interactions.

Glu-75 and Glu-135 have favorable, short-range (<4 Å) Coulomb interactions with basic groups [Table I in Supporting Information, Fig. 5(b,c)], and they are in what appear to be fairly rigid parts of the protein (low *B*-factors and standard deviation for the distance of these Coulomb interactions <0.2 Å). In 0.1*M* salt, the pK_a value of Glu-75 was shifted by 1.1 units relative to the normal pK_a value, as expected from a strong Coulomb interaction. In 1*M* salt, the shift was only 0.3, consistent with the screening of a strong favorable interaction with His-121 (Table II). The energetics of the pairwise interaction between Glu-75 and His-121 are complex, as both are members of an extensive electrostatic and hydrogen bonding network [Fig. 5(c)].[73] Notably, the resonance of Glu-75 is broadened as a result of methylene proton relaxation or conformational exchange broadening. We speculate this may be due to the complexity of interactions involving Glu-75. In contrast to the high salt sensitivity of Glu-75, the pK_a of Glu-135 was shifted relative to its normal value of 4.35 in water by only 0.6 and 0.3 units at 0.1 and 1*M* salt, respectively. The interaction between Arg-105 and Glu-135 observed in the crystal is apparently not present in solution. At 0.1*M* KCl, the Cβ resonance of Arg-105 reports an apparent pK_a of 4.3 that is not consistent with the pK_a of 3.76 of Glu-135. Arg-105 appears to be sensitive to some sort of structural rearrangement at pH 4.3, before the titration of Glu-135.

In summary, the data suggest that short-range Coulomb interactions observed in the crystal structures do not contribute significantly toward the pK_a values of carboxylic groups. The crystal structure of the protein near neutral pH might not be representative of the conformation of the protein in solution and under acidic conditions.

Complex interactions in the active site

The elevated pK_a of 6.5 for Asp-21 is highly unusual for a surface residue. Asp-21 is part of a cluster of carboxylic residues at the active site. Its carboxyl oxygens are within 5.5 Å of the carboxyl oxygens of Asp-19, Asp-40, and Glu-43 (Table I in Supporting Information). In contrast with the pK_a of Asp-21, the pK_a of Asp-19 was 2.21 and Asp-40 and Glu-43 titrated with normal pK_a values in 0.1 and 1*M* salt. The titration of Asp-21 in both 0.1 and 1*M* salt is reflected in the pH dependence of resonances of groups as far as 12 Å from Asp-21 [Table IV and Fig. 6(a)]. With the exception of His-8, which has a pK_a of 6.5,[74] no other ionizable group in SNase titrates with a pK_a near 6.5. The titration of Asp-21 is also reflected in the Cγ titration of Asp-19 (see Fig. 3) and in the titration curves of Asp-19 and Asp-40 monitored by the Hβ resonances (Supporting Information). Additional resonances that reflect the titration of Asp-21 include the H^N resonances of Gly-20, Asp-21, Thr-41, Ser-59, Ala-90, and Lys-110, the Cα resonance of Leu-36, and the Cβ resonance of Ala-109. All resonances exhibit at least a 0.1 ppm change in chemical shift owing to the titration of Asp-21.

The factors that govern the unusual pK_a value of Asp-21 are not obvious from inspection of the crystal structure. The carboxylic groups in the active site region are each within 6 Å of at least two others, and they each make several polar interactions with backbone and side chain atoms (Table I in Supporting Information). The carboxyl oxygen atoms of Asp-19 and Asp-21 have similar average solvent accessibilities of 18 and 16%, respectively. The most direct evidence that the acidic groups in the active site are in Coulomb contact comes from the low Hill coefficients of Asp-40, Glu-43, and Glu-52 titrations (Table II) in both 0.1 and 1*M* salt. Despite having four short-range repulsive Coulomb interactions and no favorable ones, Glu-43 has a normal pK_a (Table I in

Table IV
Resonances that Reflect the Titration of Asp-21

	0.1*M* KCl		1*M* KCl	
Resonance[a]	Δδ (ppm)[b]	pH_{mid}[c]	Δδ (ppm)	pH_{mid}
Gly-20 H^N	0.21	6.44 ± 0.04	0.18	5.98 ± 0.02
Asp-21 H^N	0.10	6.67 ± 0.10	0.09	5.98 ± 0.08
Leu-36 Cα	−0.54	6.41 ± 0.13	–	–
Thr-41 H^N	1.15	6.42 ± 0.01	1.06	5.95 ± 0.03
Ser-59 H^N	−0.17	6.43 ± 0.08	−0.14	6.10 ± 0.12
Ala-90 H^N	0.23	6.52 ± 0.06	0.16	6.12 ± 0.08
Ala-109 Cβ	−0.42	6.38 ± 0.11	–	–
Lys-110 H^N	0.21	6.10 ± 0.06	0.11	5.89 ± 0.16

[a] Cα and Cβ titrations were collected only at 0.1*M* KCl and 298 K; H^N titrations were collected at either 0.1*M* KCl and 298 K or 1*M* KCl and 308 K. Titration curves are supplied in Supporting Information.
[b] Amplitude ($\delta_{A-} - \delta_{AH}$) of transition associated with the titration of Asp-21.
[c] The pH_{mid} is the apparent pK_a value reported from fitting the titration curve to Eq. (1) or (2).

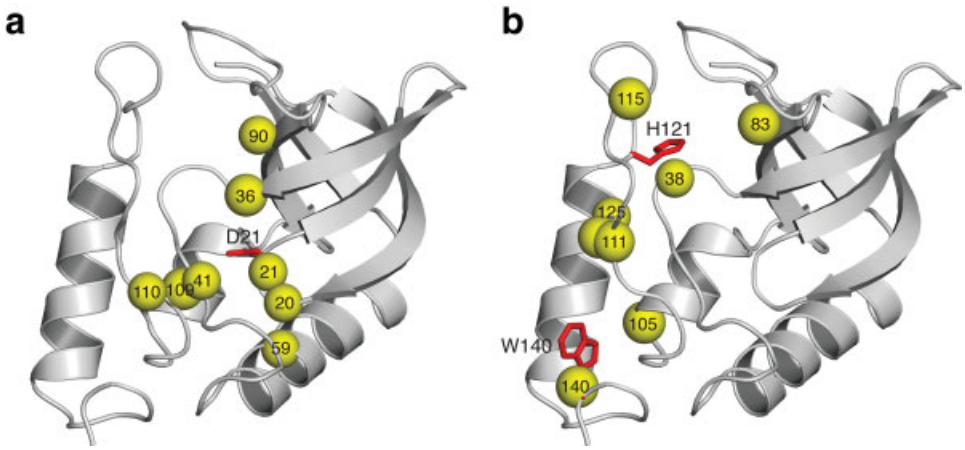

Figure 6

Atoms that sense the titrations of Asp-21 or the predenaturational transition. (**a**) atoms (yellow spheres) that sense the titration of Asp-21 (Table IV), and (**b**) atoms (yellow spheres) that report a slight predenaturational transition centered at pH 4.3 (Table V). Because hydrogen atoms are not resolved in the crystal structure, the H^N and Hγ resonances are denoted by spheres on the adjacent N and Cγ atoms, respectively.

Supporting Information). The conformation of the side chains of these carboxylic residues in the crystal structures is sensitive to the presence or absence of ligand, suggesting that these groups are in complex dynamic equilibrium. It is clear that the titrations of these four carboxylic groups are coupled to each other, but the physical nature of this coupling is not obvious from the data at hand. Similar complex interactions have been observed previously in the active sites of other proteins, such as RNase HI[58] and xylanase,[75,76] and in the NMR titration data of many proteins.[76]

pH-dependent structural changes

No large and obvious structural changes were observed between pH 8.5 and the onset of global acid unfolding at pH 2.5 (see Fig. 4). A small subset of 16 Cα, Cβ, and H^N resonances (out of 400) have pH-dependent chemical shifts that are not related to the titration of an Asp, Glu, or His residue in an obvious way. The pH dependence of one Cα resonance (Tyr-54) and four Cβ resonances (Asn-51, Lys-63, Met-65, and Ile-72) can potentially be attributed to fraying events near the α1 helix at low pH. The remaining 11 resonances are from nuclei scattered throughout the interface between the α3 helix and the remainder of the protein [Fig. 6(b) and Table V]. Most of these resonances shift at a pH below 5, with a majority exhibiting pH_{mid} values between 4.0 and 5.0 (Table V). These resonances are reporting on a subtle predenaturational transition centered at pH 4.3, which is also monitored through the pH sensitivity of the steady-state fluorescence from Trp-140.[77] In this region of the protein only Glu-43 and Glu-142 titrated with pK_a values close to 4.3. However, Glu-43 is more than 16 Å from Trp-140, and Glu-142 is in a disordered region, and it is not obvious how they could be triggering the subtle conformational change above pH 4. The subtle pH-driven conformational rearrangement detected in the NMR experiments is more likely to be related to the ionization of His-121, which is located at the N-terminus of the α3 helix and has a pK_a of 5.25.[72,73,78]

Implications for structure-based continuum electrostatics calculations

The similarity between the pK_a values of carboxylic groups in SNase and the normal pK_a values of Asp and Glu residues in water is difficult to reproduce with continuum electrostatics calculations applied to static structures. The magnitude of the shifts in pK_a values tends to be overestimated in these type of calculations.[79,80] The flexibility of side chains[12,13,81] and of the backbone,[82]

Table V

Resonances Sensitive to the Predenaturational Transition

Resonance[a]	Δδ (ppm)[b]	pH_{mid}[c]
Leu-38 H^N	−0.49	4.15 ± 0.02
Asp-83 Hβ2	−0.08	4.06 ± 0.13
Arg-105 Cα	−0.60	4.35 ± 0.07
Val-111 Cα	1.18	4.02 ± 0.11
Val-111 Cβ	−0.53	4.13 ± 0.13
Tyr-115 Cβ	0.47	4.44 ± 0.13
Leu-125 H^N	0.60	4.86 ± 0.02
Trp-140 Cβ	0.37	5.00 ± 0.13

[a]Listed are those H^N, Cα, and Cβ titrations with a pH_{mid} that coincides with the pH_{mid} (4.3) of the predenaturational transition as observed by Trp-140 fluorescence at 0.1*M* salt and 298 K. The titration curves are supplied in Supporting Information.

[b]The amplitude ($\delta_{A-} - \delta_{AH}$) of the titration associated with the predenaturational transition.

[c]The pH_{mid} is the apparent pK_a value reported from fitting the titration curve to Eq. (1).

which are difficult to treat computationally, is thought to be partly responsible for the relatively weak magnitude of electrostatic effects at the protein–water interface. Some of the methods that have been proposed to improve continuum calculations involve use of arbitrarily high protein dielectric constants,[12,17,48] explicit treatment of flexibility of side chains with Monte Carlo methods,[13] or with molecular dynamics simulations.[19,83,84] In practice, the flexibility of the backbone is difficult to simulate, whereas explicit treatment of side chain flexibility has already been shown to improve pK_a calculations.[13,85]

We have shown previously that continuum calculations based on the numerical solution of the linearized Poisson-Boltzmann equation with finite difference methods reproduce the pairwise Coulomb contributions to the pK_a values of histidines in SNase when the static protein is treated with an artificially high dielectric constant of 20,[72,73] but they fail to reproduce the acid unfolding of this protein. Acid unfolding is governed primarily by the difference in the pK_a values of the carboxylic groups in the native and in the acid-unfolded states.[17] The problem is that the calculated pK_a values of carboxylic groups in the native state are too depressed owing to the exaggeration of Coulomb interactions with basic groups. The data in this study suggest that the failure of the calculations might reflect the fact that the crystal structure is not a faithful representation of the ensemble of the protein in solution at all pH values.

To examine the inability of FDPB calculations to reproduce the pK_a values of Asp and Glu residues when applied to static structures, we compared measured and calculated pK_a values (see Fig. 7). To demonstrate the high sensitivity of the calculations to the crystal structures used, the calculations were performed with the structure of the wild-type protein, with the structure of the Δ+PHS protein, and also with a model of the Δ+PHS structure obtained from the Δ+PHS/V66K variant. Figure 7(a–d) illustrates the problems with FDPB calculations. In general, the calculated pK_a values of Asp and Glu residues are lower than the measured ones. Even when the protein was treated with a high dielectric constant of 20 [Fig. 7(a,c)], Coulomb interactions between acidic and basic residues are exaggerated, and the calcu-

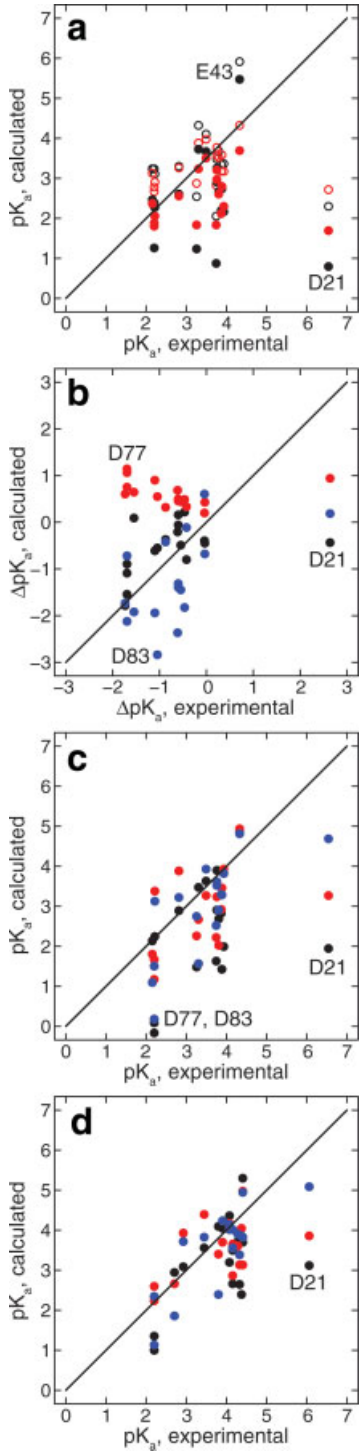

Figure 7

Correlation between experimental and calculated pK_a values. (**a**) Correlation between experimental pK_a values in 0.1*M* salt and values calculated with FDPB/SS using ε_{in} = 20 (closed black circle) and ε_{in} = 78.5 (closed red circle) in 0.1*M* ionic strength, and ε_{in} = 20 (open black circle) and ε_{in} = 80 (open red circle) in 1.0*M* ionic strength. These calculations were performed with the 1stn structure.[45] (**b**) Correlation between measured shifts in pK_a values relative to the model compound values in Table II at 0.1*M* salt, and contributions to the calculated shifts from background (closed black circle), Born (closed red circle), and Coulomb (closed blue circle) terms, calculated with the FDPB/FULL method using ε_{in} = 20 and 0.1*M* ionic strength. This calculation was performed with the crystal structure of Δ+PHS. (**c**) Correlation between experimental pK_a values measured in 0.1*M* salt and values calculated using FDPB/FULL with ε_{in} = 20 using the structure of the wild type (closed black circle), the structure of Δ+PHS modeled from its V66K variant described previously[23] (closed red circle), and the crystal structure of Δ+PHS (closed blue circle). (**d**) Same as (c) but in 1.0*M* ionic strength.

lated pK_a values are more depressed than the experimental values. The disagreement persisted even when the protein was treated with the dielectric constant of water (ε_{in} = 78.5). The agreement is best in 1*M* ionic strength [Fig. 7(a,d)], when Coulomb interactions are highly screened.

To establish that the problem stems from exaggeration of the calculated Coulomb effects, the shifts in calculated pK_a values were parsed into contributions from Coulomb and from non-Coulomb effects. The data in Figure 7(b) show that Coulomb contributions to the calculated pK_a values are large, whereas the self-energy term contributes weakly to the calculated pK_a values because the destabilizing Born term is usually offset by stabilizing contributions from interactions with permanent dipoles. The same conclusions are found regardless of whether the simplified "single site" [Fig. 7(a)] or the more realistic "full-site" [Fig. 7(c)] method is used in the calculations.[17] The contributions to shifts in pK_a values from interactions between the ionizable groups and nearby polar groups (background term contributions) correlate quite well with the measured pK_a values. This is consistent with the idea that pK_a values of carboxylic groups are governed primarily by interactions with polar groups.[14,66]

The data in Figure 7(c) illustrate that the problems with the calculations are not related to the specific structure used. Although the pK_a values calculated with the crystal structure of the Δ+PHS protein used in the NMR experiments are in closer agreement with the measured pK_a values than the values calculated with the structure of the wild-type protein or with the model structure of Δ+PHS made from its V66K variant, the problems persist independently of the structure used in the calculations. These results are fully consistent with previous observations that structure-based pK_a calculations with static structure are highly sensitive to the structure used, even when the structures are highly similar, and even when the protein is treated with high dielectric constants.[17]

Treatment of the protein interior with the dielectric constant of water (ε_{in} = 78.5) did not improve the agreement between the experimental and calculated pK_a values [Fig. 7(a)]. In these calculations, the dehydration penalty is zero and the magnitude of interactions between ionizable groups and polar groups is greatly reduced. However, even in these calculations, the net Coulomb interactions are too strong, and the calculated pK_a values are still too depressed. This problem is minimized in 1*M* ionic strength, where medium- and long-range interactions are almost completely screened [Fig. 7(d)].

The results from the calculations that treat the protein interior with ε_{in} = 78.5 have important implications in understanding the source of the discrepancy between the experimental and calculated pK_a values. At such high dielectric constants, continuum-based calculations can become insensitive to the details of their implementation because electrostatic energies are largely attenuated. In previous work, it was found that empirical adjustments of many parameters including charge set, tautomeric state, and so forth did not improve the calculations.[17] Although these observations do not eliminate systematic errors from continuum-based calculations as a possible source of the observed discrepancy in pK_a values, they leave room for another interpretation: the structures used in the calculations do not represent well the ensemble of structures in solution. Explicit relaxation of the structure in the calculations may improve the agreement between the calculated and experimental pK_a values. However, the nature of the relaxation must be subtle because no evidence was uncovered by NMR spectroscopy for a major pH-dependent structural change. Asp and Glu residues in SNase are typically found at the ends of elements of secondary structure (see Fig. 1). Fraying of these elements may contribute to local fluctuations that expose Asp and Glu residues to bulk water, leading to a normalization of pK_a values toward values comparable to those of model compounds in water. Additional NMR spectroscopy experiments will be necessary to monitor structural changes.

Differences in the salt dependence of the pK_a of acidic and basic residues in water

Structure-based calculations with continuum methods will have to be modified to account for differences in the salt dependence of the pK_a values of amines and carboxylic groups in water. The calculated ionic strength dependence of the solvation energies of Asp and Glu residues in model compounds in water are comparable to those calculated previously[60] for model histidines in water (see Fig. 8). These solvation energies were calculated with the FDPB method as the difference in the self-energy of the charged and neutral forms of the blocked residue in vacuum and in solution. The pK_a values in Figure 8 were calculated relative to the pK_a values measured for the model compound in water (Asp, 3.90; Glu, 4.35; His, 6.46) in 0.1*M* KCl (0.2*M* KCl for His). Over the range of ionic strength 0.01 to 1.0*M*, the calculated pK_a values of histidines shift up by 0.15 units, and the pK_a values of carboxylic groups shift down by the same amount (0.17). The calculated ionic strength dependence is consistent with the experimental measurements for His model compounds in water, but it contradicts measurements with Asp and Glu. Asp and Glu residues appear to be insensitive to salt over this range of concentration. Because the effect of ionic strength on solvation energies is not treated explicitly in pK_a calculations, the salt dependence of Asp and Glu residues with standard FDPB methods is calculated correctly, but the salt dependence of amines will be in error because the effect shown in Figure 8 is not normally taken into account. Note that although the effects of salt on the pK_a values of model compounds are modest, the cumulative effect of many

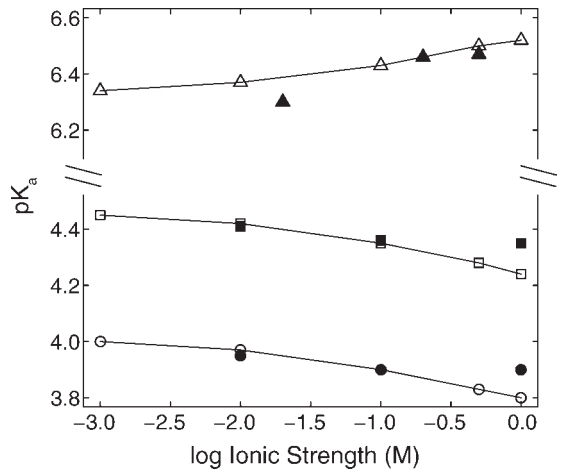

Figure 8

Calculated effect of ionic strength on the pK_a of Asp (○), Glu (□), and His (Δ) residues in model compounds in water. Experimental and calculated pK_a values are represented by filled and open symbols, respectively. The pK_a values were calculated relative to the experimental pK_a values of 3.90, 4.35, and 6.46 for Asp, Glu, and His,[60] respectively, measured with NMR spectroscopy in 0.1*M* KCl (0.2*M* KCl for His). The shift in the calculated data reflects the ionic strength dependence of the hydration energies.

small shifts in the pK_a of many ionizable groups can give rise to a substantial effect.

We speculate that the difference in the intrinsic salt sensitivity of the pK_a of amines and carboxylic residues reflects differences in their hydration properties and in the hydration properties of their counterions.[86–88] The oxygen atoms in carboxylic groups are always well hydrated and so are their countercations. Because both the negatively charged carboxylic oxygen atoms and the countercations remain fully hydrated, they never approach each other closely, thereby minimizing interactions that would promote the charged form of the carboxylic group over the neutral one (i.e., a downward shift in pK_a never occurs). In contrast, amines and chloride ions are more poorly hydrated, thus they can establish favorable, weak complexes that promote the charged form of the amine (i.e., the pK_a of the amine increases with increasing ionic strength).

Accuracy of calculated and measured pK_a values

To assess how small errors in the calculated pK_a values of many groups can cloud the interpretation of global pH-dependent properties of proteins, the overall H^+ titration curve measured with direct potentiometric methods[49] was compared with H^+ titration curves obtained from the NMR data and from the FDPB calculations (see Fig. 9). The overall H^+ binding isotherm obtained from the NMR data was calculated as a sum of the individual site-isotherms using the pK_a values measured with NMR spectroscopy and the extracted Hill coefficients to adjust the slopes of the titration curves. The agreement between the global H^+ binding curve measured potentiometrically and the one measured from the experimental pK_a values was excellent, underscoring the high accuracy and precision of the titration curves measured with NMR spectroscopy. These two curves overlap over a wide range of pH. They begin to deviate at pH < 3, where the cooperative acid unfolding of the protein begins. In contrast, the best overall H^+ titration curve that could be calculated with FDPB electrostatics is considerably different from the experimental curve, as noted previously.[49] In the calculations that come closest to reproducing the experimental data, the average difference between calculated and measured pK_a values of carboxylic groups is at least 0.5 pK_a units [Fig. 7(a)]. The relatively small inaccuracies in the calculated pK_a values of an individual group, summed over many groups, translate into a significant global failure. For this reason, continuum electrostatics calculations cannot yet reproduce the global H^+-driven conformational transitions of proteins.

CONCLUSIONS

The NMR data demonstrate conclusively that pK_a values of carboxylic groups calculated with continuum methods applied to static structures are too depressed

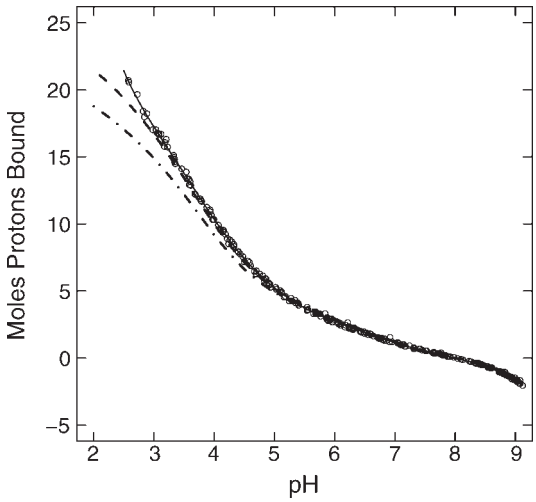

Figure 9

H^+ titration curve of Δ+PHS in 0.1*M* KCl measured potentiometrically[57] (circles and solid line), H^+ titration curve obtained from the pK_a values and Hill parameters determined with NMR spectroscopy (dashed line), and H^+ titration curve calculated with the FDPB method using the full charge implementation and the crystal structure of Δ+PHS with $\varepsilon_{in} = 20$ (dot-dashed line). The data were all zeroed arbitrarily at pH 8 for purposes of comparison. The pK_a values of the N- and C-termini were assumed to be 7.4 and 3.5, respectively. The pK_a values used for His-8 and His-121 were 6.50 and 5.24, respectively, measured previously with ^{1}H-NMR spectroscopy.[74]

even when the protein interior is treated with the dielectric constant of water. One interpretation of this observation is that the distances between ionizable moieties in the crystal structure are not representative of average distances in solution. The NMR spectroscopy experiments, which were based solely on the analysis of chemical shifts, revealed no evidence of any significant structural reorganization with decreasing pH. Although structural changes could be monitored in greater detail with other types of measurements with NMR spectroscopy (e.g., RDCs or NOEs), the data obtained thus far support the conjecture that the continuum calculations fail partly because the crystal structure of SNase is not a good representation of the native state ensemble in solution. The results from these NMR spectroscopy studies further highlight the need for computational methods for pK_a calculations that treat protein flexibility and reorganization explicitly.[13,19,89,90]

One of the methods that has been tested recently is the ensemble-modulated continuum electrostatics model that was used to analyze the acid-unfolding properties of SNase.[82] In this approach, the protein is modeled as a large ensemble of structures. Different segments in the different structures that constitute the ensemble are treated thermodynamically as if they were locally unfolded. In these calculations, the probability of local unfolding is coupled to changes in pH because the pK_a values of the ionizable groups are allowed to have different values when they are in folded or in unfolded segments of a structure. With this model, it is possible to determine how the population of the ensemble changes with pH. These ensemble-based calculations identified a set of Asp and Glu residues in SNase that were predicted to titrate with normal pK_a values because they are in locally unstable regions of the protein that are prone to unfolding, especially under increasingly acidic conditions. They also identified a set of Asp and Glu residues that have depressed pK_a values and which are thought to be responsible for H^+ uptake upon acid unfolding. These groups are found in regions of the protein that are less prone to undergo local unfolding as the concentration of H^+ increases with decreasing pH. The present NMR studies are largely consistent with the results of these ensemble calculations. However, the NMR spectroscopy data did not contribute any direct support to the idea that the pK_a values reflect the intrinsic stability of the local microenvironments around ionizable groups. No evidence has been found of any significant local structural reorganization coupled to changes in pH.

ACKNOWLEDGMENTS

The authors gratefully acknowledge the Johns Hopkins University Biomolecular NMR facility for technical expertise and the use of their spectrometers. They also thank Prof. Juliette Lecomte for valuable discussions and insights.

REFERENCES

1. Chu AH, Turner BW, Ackers GK. Effects of protons on the oxygenation-linked subunit assembly in human hemoglobin. Biochemistry 1984;23:604–617.
2. Baker D, Agard DA. Influenza hemagglutinin—kinetic control of protein function. Structure 1994;2:907–910.
3. Ehrlich LS, Liu T, Scarlata S, Chu B, Carter CA. HIV-1 capsid protein forms spherical (immature-like) and tubular (mature-like) particles in vitro: structure switching by pH-induced conformational changes. Biophys J 2001;81:586–594.
4. Krantz BA, Trivedi AD, Cunningham K, Christensen KA, Collier RJ. Acid-induced unfolding of the amino-terminal domains of the lethal and edema factors of anthrax toxin. J Mol Biol 2004;344:739–756.
5. Forsyth WR, Antosiewiez JM, Robertson AD. Empirical relationships between protein structure and carboxyl p*K*(a) values in proteins. Proteins: Struct Funct Genet 2002;48:388–403.
6. Edgcomb SP, Murphy KP. Variability in the p*K*(a) of histidine side-chains correlates with burial within proteins. Proteins: Struct Funct Genet 2002;49:1–6.
7. Tanford C, Kirkwood JG. Theory of protein titration curves. I. General equations for impenetrable spheres. J Am Chem Soc 1957;79:5333–5339.
8. Matthew JB, Gurd FRN, Garcia-Moreno EB, Flanagan MA, March KL, Shire SJ. pH-dependent processes in proteins. CRC Crit Rev Biochem 1985;18:91–197.
9. Klapper I, Hagstrom R, Fine R, Sharp K, Honig B. Focusing of electric fields in the active site of Cu-Zn superoxide dismutase: effects of ionic strength and amino-acid modification. Proteins: Struct Funct Genet 1986;1:47–59.
10. Bashford D, Karplus M. p*K*(a)s of ionizable groups in proteins—atomic detail from a continuum electrostatic model. Biochemistry 1990;29:10219–10225.
11. Karshikoff A. A simple algorithm for the calculation of multiple-site titration curves. Protein Eng 1995;8:243–248.
12. Antosiewicz J, McCammon JA, Gilson MK. The determinants of p*K*(a)s in proteins. Biochemistry 1996;35:7819–7833.
13. Alexov EG, Gunner MR. Incorporating protein conformational flexibility into the calculation of pH-dependent protein properties. Biophys J 1997;72:2075–2093.
14. Li H, Robertson AD, Jensen JH. Very fast empirical prediction and rationalization of protein p*K*(a) values. Proteins: Struct Funct Bioinformatics 2005;61:704–721.
15. Warshel A, Sharma PK, Kato M, Parson WW. Modeling electrostatic effects in proteins. Biochim Biophys Acta 2006;1764:1647–1676.
16. Kieseritzky G, Knapp E-W. Optimizing p*K*(a) computation in proteins with pH adapted conformations. Proteins: Struct Funct Bioinformatics 2008;71:1335–1348.
17. Fitch CA, Whitten ST, Hilser VJ, Garcia-Moreno B. Molecular mechanisms of pH-driven conformational transitions of proteins: insights from continuum electrostatics calculations of acid unfolding. Proteins: Struct Funct Bioinformatics 2006;63:113–126.
18. Whitten ST, Garcia-Moreno B. pH dependence of stability of staphylococcal nuclease: evidence of substantial electrostatic interactions in the denatured state. Biochemistry 2000;39:14292–14304.
19. van Vlijmen HWT, Schaefer M, Karplus M. Improving the accuracy of protein p*K*(a) calculations: conformational averaging versus the average structure. Proteins: Struct Funct Genet 1998;33:145–158.
20. Nielsen JE, Andersen KV, Honig B, Hooft RWW, Klebe G, Vriend G, Wade RC. Improving macromolecular electrostatics calculations. Protein Eng 1999;12:657–662.

21. Warshel A, Levitt M. Theoretical studies of enzymic reactions—dielectric, electrostatic and steric stabilization of carbonium-ion in reaction of lysozyme. J Mol Biol 1976;103:227–249.
22. Nielsen JE, Vriend G. Optimizing the hydrogen-bond network in Poisson-Boltzmann equation-based p*K*(a) calculations. Proteins: Struct Funct Genet 2001;43:403–412.
23. Garcia-Moreno B, Dwyer JJ, Gittis AG, Lattman EE, Spencer DS, Stites WE. Experimental measurement of the effective dielectric in the hydrophobic core of a protein. Biophys Chem 1997;64:211–224.
24. Shortle D, Meeker AK. Mutant forms of staphylococcal nuclease with altered patterns of guanidine hydrochloride and urea denaturation. Proteins: Struct Funct Genet 1986;1:81–89.
25. Fuchs S, Cuatrecasas P, Anfinsen CB. An improved method for purification of staphylococcal nuclease. J Biol Chem 1967;242:4768–4770.
26. SAINT V6.63. Program for reduction of area detector data. Madison, WI: BRUKER AXS Inc, 2000.
27. Nguyen DM, Reynald RL, Gittis AG, Lattman EE. X-ray and thermodynamic studies of staphylococcal nuclease variants I92E and I92K: insights into polarity of the protein interior. J Mol Biol 2004;341:565–574.
28. McCoy AJ, Grosse-Kunstleve RW, Storoni LC, Read RJ. Likelihood-enhanced fast translation functions. Acta Crystallogr D Biol Crystallogr 2005;61:458–464.
29. Bailey S. The CCP4 suite—programs for protein crystallography. Acta Crystallogr D Biol Crystallogr 1994;50:760–763.
30. Murshudov GN, Vagin AA, Dodson EJ. Refinement of macromolecular structures by the maximum-likelihood method. Acta Crystallogr D Biol Crystallogr 1997;53:240–255.
31. Emsley P, Cowtan K. Coot: model-building tools for molecular graphics. Acta Crystallogr D Biol Crystallogr 2004;60:2126–2132.
32. Laskowski RA, Macarthur MW, Moss DS, Thornton JM. PROCHECK—a program to check the stereochemical quality of protein structures. J Appl Crystallogr 1993;26:283–291.
33. Wishart DS, Bigam CG, Yao J, Abildgaard F, Dyson HJ, Oldfield E, Markley JL, Sykes BD. H-1, C-13 and N-15 chemical shift referencing in biomolecular NMR. J Biomol NMR 1995;6:135–140.
34. Wittekind M, Mueller L. HNCACB, a high-sensitivity 3D NMR experiment to correlate amide-proton and nitrogen resonances with the α-carbon and β-carbon resonances in proteins. J Magn Reson B 1993;101:201–205.
35. Grzesiek S, Bax A. Correlating backbone amide and side chain resonances in larger proteins by multiple relayed triple resonance NMR. J Am Chem Soc 1992;114:6291–6293.
36. Grzesiek S, Bax A. An efficient experiment for sequential backbone assignment of medium-sized isotopically enriched proteins. J Magn Reson 1992;99:201–207.
37. Grzesiek S, Anglister J, Bax A. Correlation of backbone amide and aliphatic side chain resonances in 13C/15N-enriched proteins by isotropic mixing of 13C magnetization. J Magn Reson B 1993; 101:114–119.
38. Pellecchia M, Iwai H, Szyperski T, Wuthrich K. The 2D NMR experiments H(C)CO2 and H2 for assignment and pH titration of carboxylate groups in uniformly 15N/13C-labeled proteins. J Magn Reson 1997;124:274.
39. Delaglio F, Grzesiek S, Vuister GW, Zhu G, Pfeifer J, Bax A. NMRPIPE—a multidimensional spectral processing system based on UNIX pipes. J Biomol NMR 1995;6:277–293.
40. Goddard TD, Kneller DG. SPARKY 3. San Francisco: University of California.
41. Bodenhausen G, Ruben DJ. Natural abundance N-15 NMR by enhanced heteronuclear spectroscopy. Chem Phys Lett 1980;69:185–189.
42. Team RDC. R: a language and environment for statistical computing. Vienna, Austria: R Foundation for Statistical Computing; 2007.
43. Markley JL. Observation of histidine residues in proteins by means of nuclear magnetic resonance spectroscopy. Acc Chem Res 1975;8:70–80.
44. Perez-Canadillas JM, Campos-Olivas R, Lacadena J, del Pozo AM, Gavilanes JG, Santoro J, Rico M, Bruix M. Characterization of p*K*(a) values and titration shifts in the cytotoxic ribonuclease α-sarcin by NMR. Relationship between electrostatic interactions, structure, and catalytic function. Biochemistry 1998;37:15865–15876.
45. Hynes TR, Fox RO. The crystal structure of staphylococcal nuclease refined at 1.7 A resolution. Proteins: Struct Funct Genet 1991;10: 92–105.
46. Davis ME, Madura JD, Luty BA, McCammon JA. Electrostatics and diffusion of molecules in solution–simulations with the university of Houston Brownian dynamics program. Comput Phys Commun 1991;62:187–197.
47. Madura JD, Briggs JM, Wade RC, Davis ME, Luty BA, Ilin A, Antosiewicz J, Gilson MK, Bagheri B, Scott LR, McCammon JA. Electrostatics and diffusion of molecules in solution—simulations with the University of Houston Brownian dynamics program. Comput Phys Commun 1995;91:57–95.
48. Antosiewicz J, McCammon JA, Gilson MK. Prediction of pH-dependent properties of proteins. J Mol Biol 1994;238:415–436.
49. Fitch CA, Karp DA, Lee KK, Stites WE, Lattman EE, Garcia-Moreno B. Experimental p*K*(a) values of buried residues: analysis with continuum methods and role of water penetration. Biophys J 2002;82:3289–3304.
50. Brooks BR, Bruccoleri RE, Olafson BD, States DJ, Swaminathan S, Karplus M. CHARMM—a program for macromolecular energy, minimization, and dynamics calculations. J Comput Chem 1983; 4:187–217.
51. Gilson MK. Multiple-site titration and molecular modelling—2 rapid methods for computing energies and forces for ionizable groups in proteins. Proteins: Struct Funct Genet 1993;15:266–282.
52. Warshel A. Calculations of enzymic reactions: calculations of p*K*(a), proton transfer reactions, and general acid catalysis reactions in enzymes. Biochemistry 1981;20:3167–3177.
53. Antosiewicz J, Briggs JM, Elcock AH, Gilson MK, McCammon JA. Computing ionization states of proteins with a detailed charge model. J Comput Chem 1996;17:1633–1644.
54. Keim P, Vigna RA, Morrow JS, Marshall RC, Gurd FRN. Carbon-13 nuclear magnetic resonance of pentapeptides of glycine containing central residues of serine, threonine, aspartic and glutamic acids, asparagine, and glutamine. J Biol Chem 1973;248:7811–7818.
55. Richarz R, Wüthrich K. Carbon-13 NMR chemical shifts of the common amino acid residues measured in aqueous solutions of the linear tetrapeptides H-Gly-Gly-X-L-Ala-OH. Biopolymers 1978;17: 2133–2141.
56. Bundi A, Wuthrich K. H-1-NMR parameters of the common amino acid residues measured in aqueous solutions of the linear tetrapeptides H-Gly-Gly-X-L-Ala-OH. Biopolymers 1979;18:285–297.
57. Karp DA, Gittis AG, Stahley MR, Fitch CA, Stites WE, Garcia-Moreno B. High apparent dielectric constant inside a protein reflects structural reorganization coupled to the ionization of an internal Asp. Biophys J 2007;92:2041–2053.
58. Oda Y, Yamazaki T, Nagayama K, Kanaya S, Kuroda Y, Nakamura H. Individual ionization constants of all the carboxyl groups in Ribonuclease HI from *Escherichia coli* determined by NMR. Biochemistry 1994;33:5275–5284.
59. Chen HA, Pfuhl M, McAlister MSB, Driscoll PC. Determination of p*K*(a) values of carboxyl groups in the N-terminal domain of rat CD2: anomalous p*K*(a) of a glutamate on the ligand-binding surface. Biochemistry 2000;39:6814–6824.
60. Kao YH, Fitch CA, Bhattacharya S, Sarkisian CJ, Lecomte JTJ, Garcia-Moreno B. Salt effects on ionization equilibria of histidines in myoglobin. Biophys J 2000;79:1637–1654.
61. Sundd M, Iverson N, Ibarra-Molero B, Sanchez-Ruiz JM, Robertson AD. Electrostatic interactions in ubiquitin: stabilization of carboxylates by lysine amino groups. Biochemistry 2002;41:7586–7596.
62. Wishart DS, Case DA. Use of chemical shifts in macromolecular structure determination. In: James TL, Dotsch V, Schmitz U, editors. Methods in enzymology, Vol. 338: Nuclear magnetic resonance of bio-

logical macromolecules, Part A. San Diego, CA: Academic Press; 2001. pp 3–34.
63. Hagen R, Roberts JD. Nuclear magnetic resonance spectroscopy—13C spectra of aliphatic carboxylic acids and carboxylate anions. J Am Chem Soc 1969;91:4504–4506.
64. Hubbard SJ, Thornton JM. NACCESS. University College London: Department of Biochemistry and Molecular Biology; 1993.
65. Li H, Robertson AD, Jensen JH. The determinants of carboxyl p*K*(a) values in turkey ovomucoid third domain. Proteins: Struct Funct Bioinformatics 2004;55:689–704.
66. Clark AT, Smith K, Muhandiram R, Edmondson SP, Shriver JW. Carboxyl p*K*(a) values, ion pairs, hydrogen bonding, and the pH-dependence of folding the hyperthermophile proteins Sac7d and Sso7d. J Mol Biol 2007;372:992–1008.
67. Bundi A, Wuthrich K. Use of amide H-1-NMR titration shifts for studies of polypeptide conformation. Biopolymers 1979;18:299–311.
68. Szyperski T, Antuch W, Schick M, Betz A, Stone SR, Wuthrich K. Transient hydrogen bonds identified on the surface of the NMR solution structure of hirudin. Biochemistry 1994;33:9303–9310.
69. McDonald IK, Thornton JM. Satisfying hydrogen-bonding potential in proteins. J Mol Biol 1994;238:777–793.
70. Thanki N, Thornton JM, Goodfellow JM. Distributions of water around amino acid residues in proteins. J Mol Biol 1988;202:637–657.
71. Dwyer JJ, Gittis AG, Karp DA, Lattman EE, Spencer DS, Stites WE, Garcia-Moreno B. High apparent dielectric constants in the interior of a protein reflect water penetration. Biophys J 2000;79:1610–1620.
72. Lee KK, Fitch CA, Lecomte JTJ, Garcia-Moreno B. Electrostatic effects in highly charged proteins: salt sensitivity of p*K*(a) values of histidines in staphylococcal nuclease. Biochemistry 2002;41:5656–5667.
73. Baran KL, Chimenti MS, Schlessman JL, Fitch CA, Herbst KJ, Garcia-Moreno BE. Electrostatic effects in a network of polar and ionizable groups in staphylococcal nuclease. J Mol Biol 2008;379:1045–1062.
74. Fitch C. Computational studies of molecular determinants of p*K*(a) values and electrostatic contributions to stability in proteins [dissertation]. Baltimore: Johns Hopkins University; 2002.
75. McIntosh LP, Hand G, Johnson PE, Joshi MD, Korner M, Plesniak LA, Ziser L, Wakarchuk WW, Withers SG. The p*K*(a) of the general acid/base carboxyl group of a glycosidase cycles during catalysis: a C-13-NMR study of *Bacillus circuluns* xylanase. Biochemistry 1996; 35:9958–9966.
76. Sondergaard CR, McIntosh LP, Pollastri G, Nielsen JE. Determination of electrostatic interaction energies and protonation state populations in enzyme active sites. J Mol Biol 2008;376:269–287.
77. Hirano S, Kamikubo H, Yamazaki Y, Kataoka M. Elucidation of information encoded in tryptophan 140 of staphylococcal nuclease. Proteins: Struct Funct Bioinformatics 2005;58:271–277.
78. Epstein HF, Schechter AN, Cohen JS. Folding of staphylococcal nuclease: magnetic resonance and fluorescence studies of individual residues. Proc Natl Acad Sci USA 1971;68:2042–2046.
79. Forsyth WR, Gilson MK, Antosiewicz J, Jaren OR, Robertson AD. Theoretical and experimental analysis of ionization equilibria in ovomucoid third domain. Biochemistry 1998;37:8643–8652.
80. Garcia-Moreno E B, Fitch CA. Structural interpretation of pH and salt-dependent processes in proteins with computational methods. In: Holt JM, Johnson ML, Ackers GK, editors. Methods in enzymology, Vol. 380. San Diego, CA: Academic Press; 2004. pp 20–51.
81. You TJ, Bashford D. Conformation and hydrogen ion titration of proteins: a continuum electrostatic model with conformational flexibility. Biophys J 1995;69:1721–1733.
82. Whitten ST, Garcia-Moreno B, Hilser VJ. Local conformational fluctuations can modulate the coupling between proton binding and global structural transitions in proteins. Proc Natl Acad Sci USA 2005;102:4282–4287.
83. Warshel A. Molecular dynamics simulations of biological reactions. Acc Chem Res 2002;35:385–395.
84. Schutz CN, Warshel A. What are the dielectric "constants" of proteins and how to validate electrostatic models? Proteins: Struct Funct Genet 2001;44:400–417.
85. Georgescu RE, Alexov EG, Gunner MR. Combining conformational flexibility and continuum electrostatics for calculating p*K*(a)s in proteins. Biophys J 2002;83:1731–1748.
86. Collins KD. Charge density-dependent strength of hydration and biological structure. Biophys J 1997;72:65–76.
87. Swanson JMJ, Maupin CM, Chen HN, Petersen MK, Xu JC, Wu YJ, Voth GA. Proton solvation and transport in aqueous and biomolecular systems: insights from computer simulations. J Phys Chem B 2007;111:4300–4314.
88. Lee S, Tikhomirova A, Shalvardjian N, Chalikian TV. Partial molar volumes and adiabatic compressibilities of unfolded protein states. Biophys Chem 2008;134:185–199.
89. Kato M, Warshel A. Using a charging coordinate in studies of ionization induced partial unfolding. J Phys Chem B 2006;110:11566–11570.
90. Chen JH, Brooks CL, Khandogin J. Recent advances in implicit solvent-based methods for biomolecular simulations. Curr Opin Struct Biol 2008;18:140–148.